THE EUROPEAN SOCIETY OF MEDICINE
Medical Research Archives, Volume 13 Issue 8

RESEARCH ARTICLE

Gut microbiota and immunometabolic response to Choline and Betaine supplementation in a Mouse Model of Diet-Induced Obesity

Néstor D. Portela[1,2], Natalia Eberhardt[3,4,#5], Gastón Bergero[3,4], Yanina L. Mazzocco[3,4], Maria P. Aoki[3,4], Cristian Galván[1,2], Roxana C. Cano[2,4], Susana A. Pesoa[1]

[1]Departamento de Diagnóstico Molecular, LACE Laboratorios, Córdoba, Argentina
[2]Unidad Asociada Área Ciencias Agrarias, In-geniería, Ciencias Biológicas y de la Salud, Consejo Nacional de Investigaciones Científicas y Tecnológicas (CONICET), Facultad de Cien-cias Químicas, Universidad Católica de Cór-doba, Córdoba, Argentina
[3]Centro de Investigaciones en Bioquímica Clí-nica e Inmunología (CIBICI), Consejo Nacional de Investigaciones Científicas y Tecnológicas (CONICET), Córdoba X5000HUA, Argentina
[4]Departamento de Bioquímica Clínica, Facultad de Ciencias Químicas, Universidad Nacional de Córdoba
[#5]Current address: Department of Medicine, Division of Cardiology, New York University, Cardiovascular Research Center, New York, University School of Medicine, New York, NY, United States

OPEN ACCESS

PUBLISHED
31 August 2025

CITATION
Portelan ND., et al., 2025. Gut microbiota and immunometabolic response to Choline and Betaine supplementation in a Mouse Model of Diet-Induced Obesity. Medical Research Archives, [online] 13(8). https://doi.org/10.18103/mra.v13i7.6877

DOI
https://doi.org/10.18103/mra.v13i7.6877

ISSN
2375-1924

ABSTRACT

Obesity is a chronic, recurring and multifactorial disease characterized by systemic inflammation, visceral adipose tissue dysfunction and gut microbiota dysbiosis. While Omega-3 fatty acids have shown beneficial effects in this context, the potential of other dietary modulators remains underexplored.

Our aim was to investigate the effects of dietary supplementation with choline and betaine on weight gain, gut microbiota composition and visceral immunometabolic profiles in a mouse model of diet-induced obesity.

Mice fed with choline and betaine supplemented diets, exhibited significantly reduced weight gain compared to obesity fat diet, at weeks 4, 12 and 24 after differential feeding was started. Beta-diversity analyses revealed sustained divergence in microbial communities between diet groups. Fat diet supplemented with choline and betaine feeding generated enrichment of SCFA-producing taxa such as *Parabacteroides, Oscillospira, Flavonifractor, Harryflintia and Christensenellaceae R7 group* while Fat diet feeding promoted the expansion of pro-inflammatory genera such as *Helicobacter* and *Negativibacillus*. In parallel, in the choline and betaine supplementation group immune data point toward an anti-inflammatory visceral adipose tissue phenotype, with IL-10–skewed T regulatory cell signatures producing high levels of IL-10.

Choline and betaine supplementation modulates the gut–adipose–immune axis by reshaping gut microbial community and enhancing host immunometabolic homeostasis. These findings support the potential of methyl-donor nutrients as dietary strategy to mitigate obesity-related inflammation and metabolic dysfunction.

Multiblock analysis with DIABLO identified a coordinated microbial–immune–metabolic signature that distinguished diet groups, linking Fat diet supplemented with choline and betaine-enriched taxa with IL-10–producing Tregs and adiponectin levels. These findings highlight the systemic impact of choline and betaine supplementation.

Keywords: Obesity, choline, betaine, gut microbiota, visceral adipose tissue, methyl donors, short-chain fatty acids, regulatory T cells, diet-induced obesity, immunometabolism

1. Introduction

Obesity is a chronic, recurring and multifactorial disease associated with systemic low-grade inflammation, metabolic dysfunction and an increased risk of non-communicable diseases[1]. A growing body of evidence implicates visceral adipose tissue (VAT) dysfunction and gut microbiota (GM) dysbiosis as critical contributors to obesity-related complications[2,3]. VAT in obesity is marked by adipocyte hypertrophy, increased infiltration of pro-inflammatory immune cells such as M1 macrophages and reduced numbers of regulatory T cells (Tregs), resulting in a pro-inflammatory microenvironment that exacerbates metabolic disturbance[3–8].

Diet is a central modulator of both GM composition and host immunometabolic responses[9–13]. In previous studies, we demonstrated that a sustained dietary supplementation with Omega-3 fatty acids modulates GM composition, favors anti-inflammatory immune profiles in VAT and improves metabolic markers in mice fed a medium-fat-content diet in a dose dependent manner[14,15]. However, the search for additional dietary components capable of exerting beneficial metabolic and immunological effects remains a priority in obesity research.

Choline and betaine are methyl-donor nutrients involved in one-carbon metabolism, epigenetic regulation and lipid homeostasis[16,17]. Both compounds have been shown to influence inflammation, lipid metabolism and intestinal barrier function. Moreover, their metabolism by the GM generates bioactive compounds that may modulate host physiology and immunity[18,19]. Despite their recognized physiological roles, the potential of choline and betaine as modulators of the gut–VAT–immune axis in the context of diet induced obesity (DIO) remains underexplored.

In the present study, we used our established medium-fat-content mouse model of obesity maintaining a constant low dosage of Omega-3 content[15], to isolate the effects of choline and betaine supplementation. We aimed to assess the impact of these compounds on the GM composition and their influence on VAT immune cell populations, with a particular focus on Tregs. Additionally, we evaluated changes in metabolic biomarkers to gain insight on the potential systemic effects of these dietary interventions.

By integrating microbiota profiling, immune phenotyping in VAT and metabolic biomarkers, this exploratory study seeks to elucidate the role of choline and betaine in shaping immunometabolic responses in obesity. Our findings may contribute to the development of novel dietary strategies aimed at restoring metabolic balance and preventing adipose tissue inflammation in obesity.

2. Materials and Methods

2.1. ANIMALS AND EXPERIMENTAL DESIGN

Male C57BL/6J (B6) mice, 6 weeks old, were obtained from the Facultad de Ciencias Veterinarias, Universidad Nacional de La Plata (Buenos Aires, Argentina). All animals were housed in isolation rooms within the Animal Facilities of the Facultad de Ciencias Químicas, Universidad Católica de Córdoba.

Mice were randomly assigned to two groups (n = 4 per group) and were allowed to acclimate to the experimental conditions for two weeks. Following this period, animals were fed for 24 weeks with one of the following diets: Obesity-Inducing Diet (FD): 11% fat, 28% protein, 4.5% crude fiber and 7.5% total minerals (TIT Can Gross) or Obesity-Inducing Diet supplemented with choline and betaine (FDCB): 16% fat, 26% protein, 3% crude fiber and 7% total minerals (Sieger Pet Foods).

All groups were maintained under standard housing conditions, including a 12-hour light/dark cycle, controlled temperature (21 ± 2 °C) and ad libitum access to food and water. Food was replaced every two days to ensure freshness.

This study was approved by the Institutional Committee for the Care and Use of Laboratory Animals (CICUAL) of the Facultad de Ciencias Químicas,

Universidad Nacional de Córdoba (Resolution No. 939, EXP-UNC: 0023836/2018). Environmental conditions were maintained according to CICUAL guidelines. All experimental procedures adhered to the Directive 2010/63/EU of the European Parliament on the protection of animals used for scientific purposes.

2.2. EVALUATION OF OBESITY DEVELOPMENT

Body weight was measured at weeks 0, 4, 12 and 24 after the start of differential feeding. DIO was defined as a body weight exceeding the mean at week 0 plus three standard deviations across all groups[20].

2.3. GUT MICROBIOTA ANALYSIS

Fecal samples were collected individually in metabolic cages at week 0, 4, 12 and 24, immediately frozen and stored at −40 °C until analysis. DNA was extracted from 220 mg of feces under sterile conditions using the QIAamp DNA Stool Mini Kit (Qiagen, Germantown, MD, USA), following the manufacturers protocol. Extracted DNA was stored at −40 °C.

Microbial profiling was conducted using the Ion 16S Metagenomics Kit and sequenced on the Ion Torrent PGM platform (Thermo Fisher Scientific). A mock community composed of ATCC bacterial strains was included as a sequencing control.

Data processing was carried out in R v4.1.2 using DADA2 (v1.22.0)[21], phyloseq (v1.38.0)[22] and microbiome (v1.16.0)[23] packages. Taxonomic assignment was based on the SILVA database v138.1[24] (updated March 2021). Sequencing data are available in the NCBI BioProject database (accession number: PRJNA1292224).

2.4. BLOOD METABOLIC PROFILE AND VAT IMMUNE CELL EVALUATION

At week 24, mice were anesthetized with inhaled isoflurane (FORANE). After 8 hours of fasting, blood was collected via cardiac puncture into heparinized tubes, centrifuged (3000 rpm, 5 min) and plasma was stored at −20 °C. Plasma concentrations of glucose, triglycerides, total cholesterol, AST, ALT, total proteins and albumin were determined using a COBAS 8000 autoanalyzer (Roche Diagnostics). Adiponectin and leptin levels were measured using ELISA kits (Abcam and Invitrogen, respectively), following the manufacturers' instructions.

Following blood collection, mice were euthanized by cervical dislocation and visceral adipose tissue (VAT) was collected for stromal vascular fraction (SVF) analysis. Epididymal adipose tissue was processed as described by Portela et al.,[15]. Surface markers included: CD11b (PeCy5), F4/80 (PeCy7), CD45 (APC) and CD4 (APC-Cy7). Intracellular markers included FOXP3 (PerCp-Cy5.5) and IL-10 (PE), following permeabilization with BD Cytofix/Cytoperm. Samples were acquired on a FACS Canto II cytometer (BD Biosciences) and data were reported as percentage of positive cells.

2.5. STATISTICAL ANALYSIS

All statistical analyses and visualizations were conducted using R software v4.1.2[25]. Data normality was assessed using the Shapiro-Wilk test. For comparisons between two groups, Student's *t*-test or Wilcoxon test was used depending on data distribution. For analyses involving more than two groups, ANOVA or Kruskal-Wallis tests were applied. When significant differences were found, post hoc pairwise comparisons were performed using the *t*-test (after ANOVA) or Wilcoxon signed-rank test (after Kruskal-Wallis), with Bonferroni correction for multiple testing. A p-value < 0.05 was considered statistically significant.

Data visualization was carried out using the ggplot2 v3.4.0[26] and ggpubr v0.5.0[27] packages.

Alpha diversity metrics (Observed ASVs, Chao1, Shannon, Simpson) and beta diversity (weighted and unweighted UniFrac) were calculated using the microbiome package v1.6.0[23]. Differences in microbiota composition between dietary groups were evaluated with ANOSIM.

Differential abundance analysis was performed using LEfSe via the microbiomeMarker package v1.9.0[28], considering features significant when LDA

scores were ≥3 and p<0.05. Correlation analyses were conducted using the corrplot package v0.92[29].

A multiblock integrative analysis was conducted using the DIABLO (Data Integration Analysis for Biomarker discovery using Latent Components) framework, implemented in the mixOmics package v6.20.0[30]. This method enabled the identification of correlated features across gut microbiota, immune, and metabolic datasets, facilitating the discrimination between dietary groups (FD vs. FDCB). Model tuning was performed through cross-validation to determine the optimal number of components and selected variables per block. Circus plots and relevance networks were used to visualize the key multi-omic correlations driving group separation.

3. Results

3.1 EFFECT OF DIETS ON THE BODY WEIGHT OF MICE

Body weight increased progressively in both groups of mice over the 24-week period, but the increase of weight in FD-fed mice was consistently higher than in FDCB fed mice (Fig. 1A). At baseline (Week 0), there was no significant difference between the two groups; however, after four weeks of differential feeding, FD-fed mice exhibited significantly higher weight than their FDCB-fed counterparts. This trend persisted at both 12 and 24 weeks (Fig. 1B). Notably, from Week 4 onward, 100% of FD-fed mice had developed obesity, whereas this proportion was only reached in the FDCB group after 24 weeks of feeding (Figure 1A).

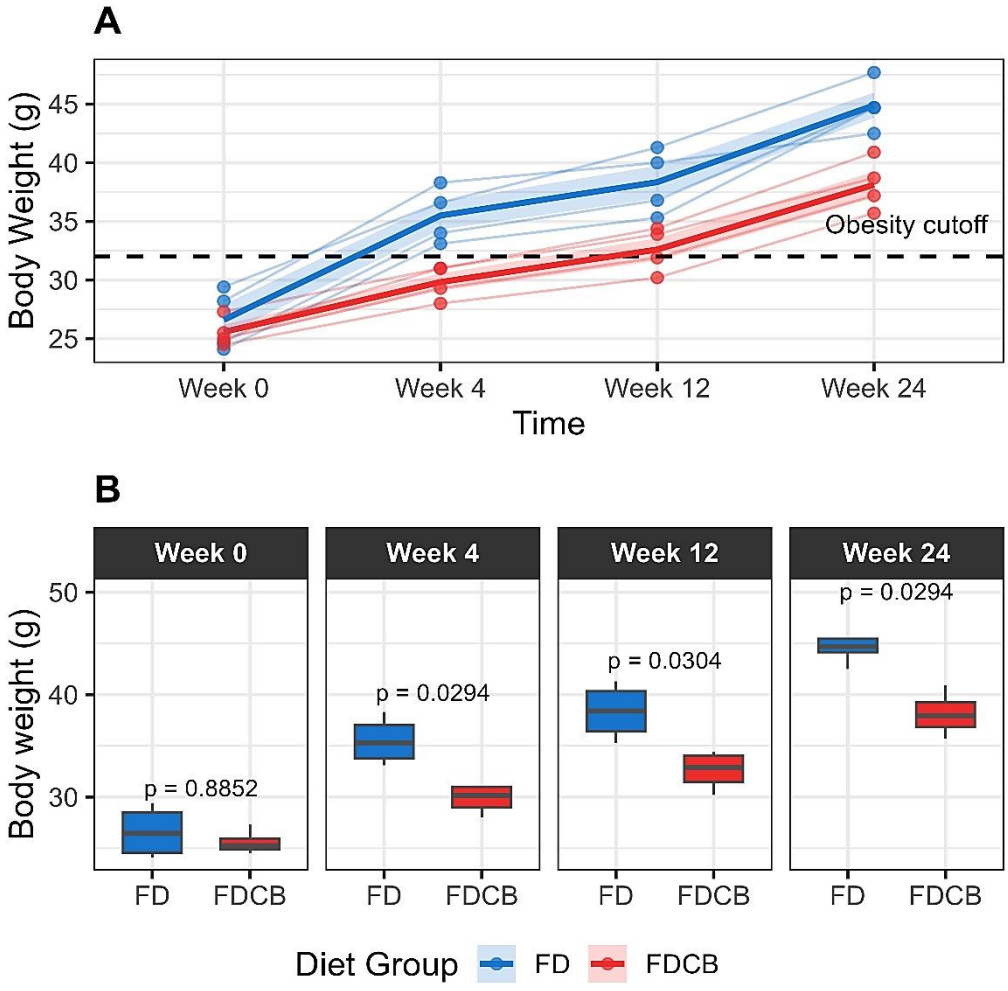

Figure 1. Body weight progression in mice over time. (**A**) Individual spaghetti plots showing body weight trajectories for each animal over 24 weeks. The mean body weight per group is overlaid as a bold line, with the shaded area representing the standard error of the mean. (**B**) Boxplots representing body weight (in grams) at each time point (Weeks 0, 4, 12 and 24) for mice fed different diets.

3.2 GUT MICROBIOTA ANALYSIS

3.2.1 Alpha diversity

A comprehensive comparison of Alpha diversity between FD and FDCB fed mice showed that, at baseline (week 0), richness metrics did not differ significantly (Observed ASVs and Chao1 indexes), while diversity indices were slightly higher in FD fed group (Shannon and Simpson). By week 4, only the Simpson index remained significantly elevated in the FD group, whereas Observed ASVs, Chao1 and Shannon, showed no differences. At Week 12, FD fed mice again displayed higher Shannon and Simpson indices, but no differences in Observed ASVs or Chao1. Finally, after 24 weeks of differential feeding, none of the Alpha diversity measures differed significantly between groups (Figure 2).

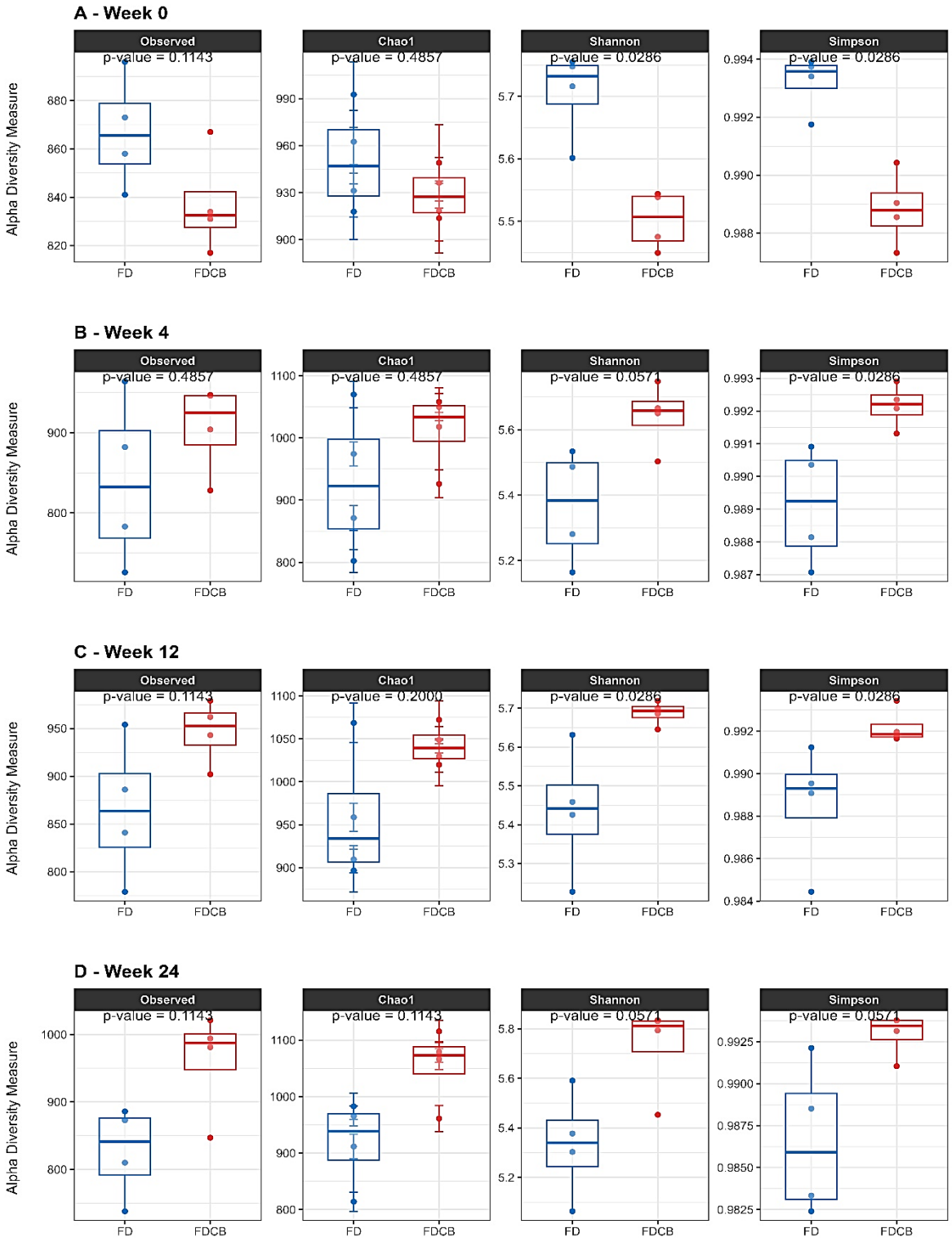

Figure 2. Alpha diversity metrics analysis. ASVs Observed, Chao1, Shannon, and Simpson at four time points: Week 0 (A), Week 4 (B), Week 12 (C) and Week 24 (D).

3.2.2 Beta diversity

To evaluate the effects of dietary choline and betaine on gut microbiota dynamics, we performed principal coordinates analysis (PCoA) using unweighted and weighted UniFrac distances at weeks 0, 4, 12 and 24. In the unweighted UniFrac PCoA (Figure 3 B, D, F, H), samples were intermixed at week 0 but formed two well-separated clusters at weeks 4, 12 and 24, indicating that presence–absence differences in low-abundance taxa underlie the diet effect. Weighted UniFrac PCoA (Figure 3 A, C, E, G), which accounts for relative abundance, also showed no grouping at baseline and clear separation at Weeks 4 and 12; however, at week 24 the clusters overlapped partially, suggesting that differences in dominant taxa had narrowed even though rare taxa continued to discriminate the diets. Supplementary Table S3 shows results of ANOSIM statistic values.

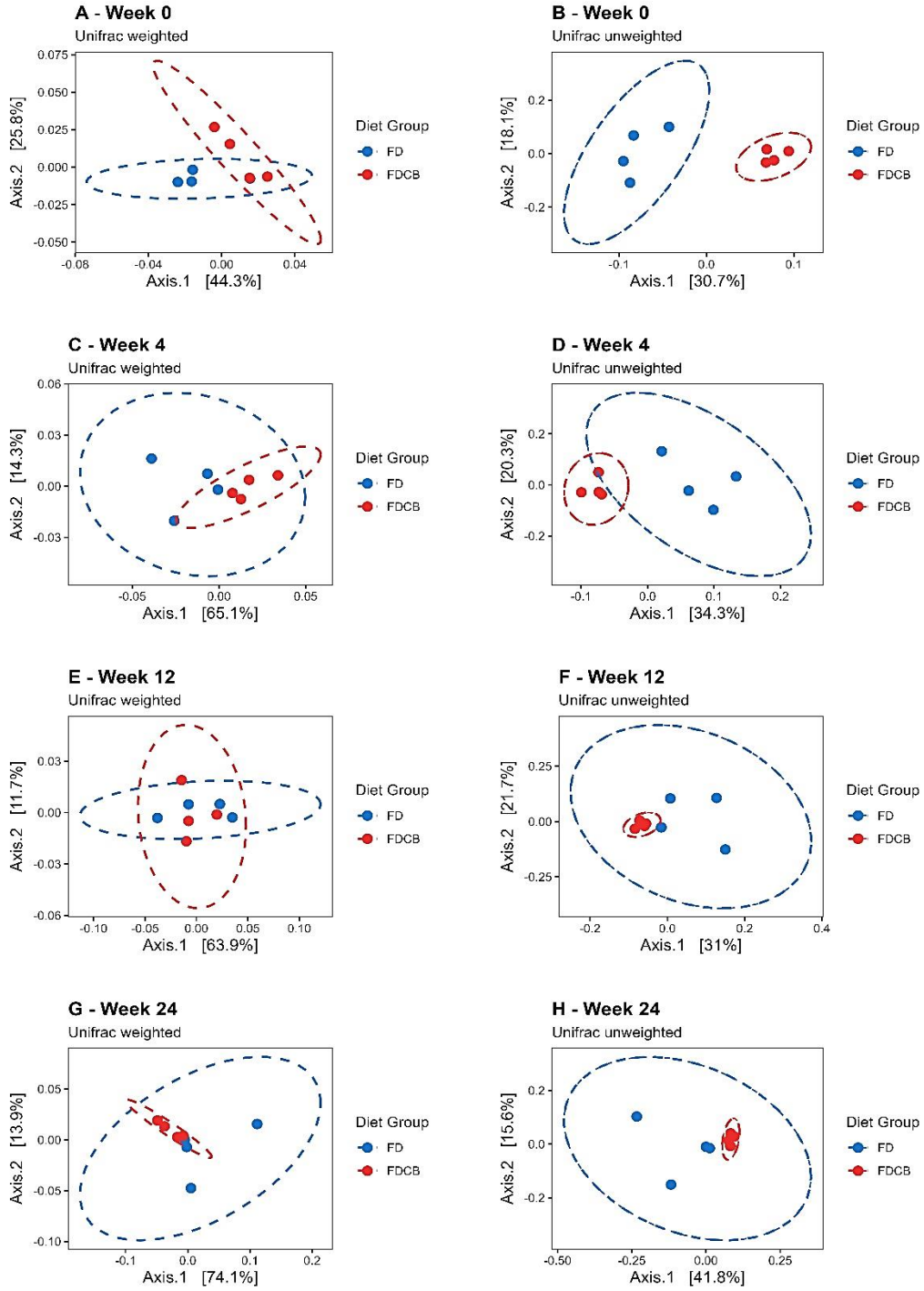

Figure 3. Principal coordinates analysis (PCoA) of beta diversity using UniFrac distances (weighted and unweighted) at weeks 0, 4, 12 and 24. Plots show the ordination of samples based on UniFrac weighted (A, C, E, G) and unweighted (B, D, F, H) distance metrics. Statistical significance of group separation was evaluated using ANOSIM (see Supplementary Table S3).

3.3 DIFFERENTIAL ANALYSIS OF GUT MICROBIOTA

Differential abundance analysis using LEfSe was performed to identify microbial biomarkers associated with diet and time. The first analysis compared the FD and FDCB diet groups at different time points (weeks 0, 4, 12 and 24). At each time point, distinct microbial features were identified as differentially abundant between the two groups. From week 4 onwards, the number and magnitude of these differences increased, indicating a progressive divergence in microbial composition between diets groups (Figure 4A-D).

The second analysis assessed longitudinal changes within each diet group. In both FD and FDCB groups, specific microbial profiles were observed at each time point. In the FD group, the most pronounced differences were detected at the later stages of the experiment. In the FDCB group, significant temporal shifts were observed, with several biomarkers unique to each time point (Figure 5A-B).

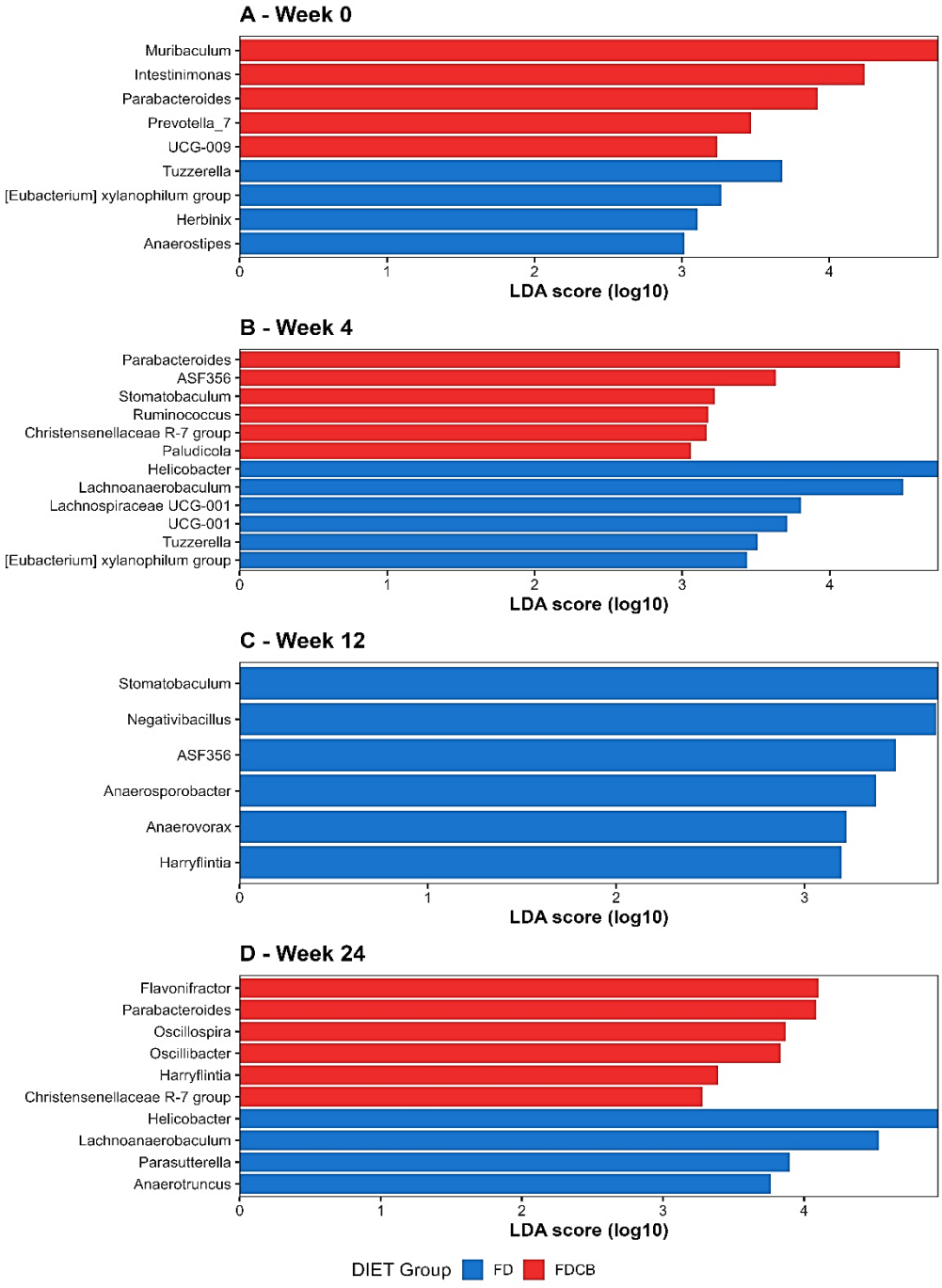

Figure 4. LEfSe (Linear Discriminant Analysis Effect Size) was used to identify bacterial genera that differed significantly between diet groups (FD vs. FDCB) at weeks 0 (A), 4 (B), 12 (C) and (24). Only taxa with a linear discriminant analysis (LDA) score >3 and p-value <0.05 are shown.

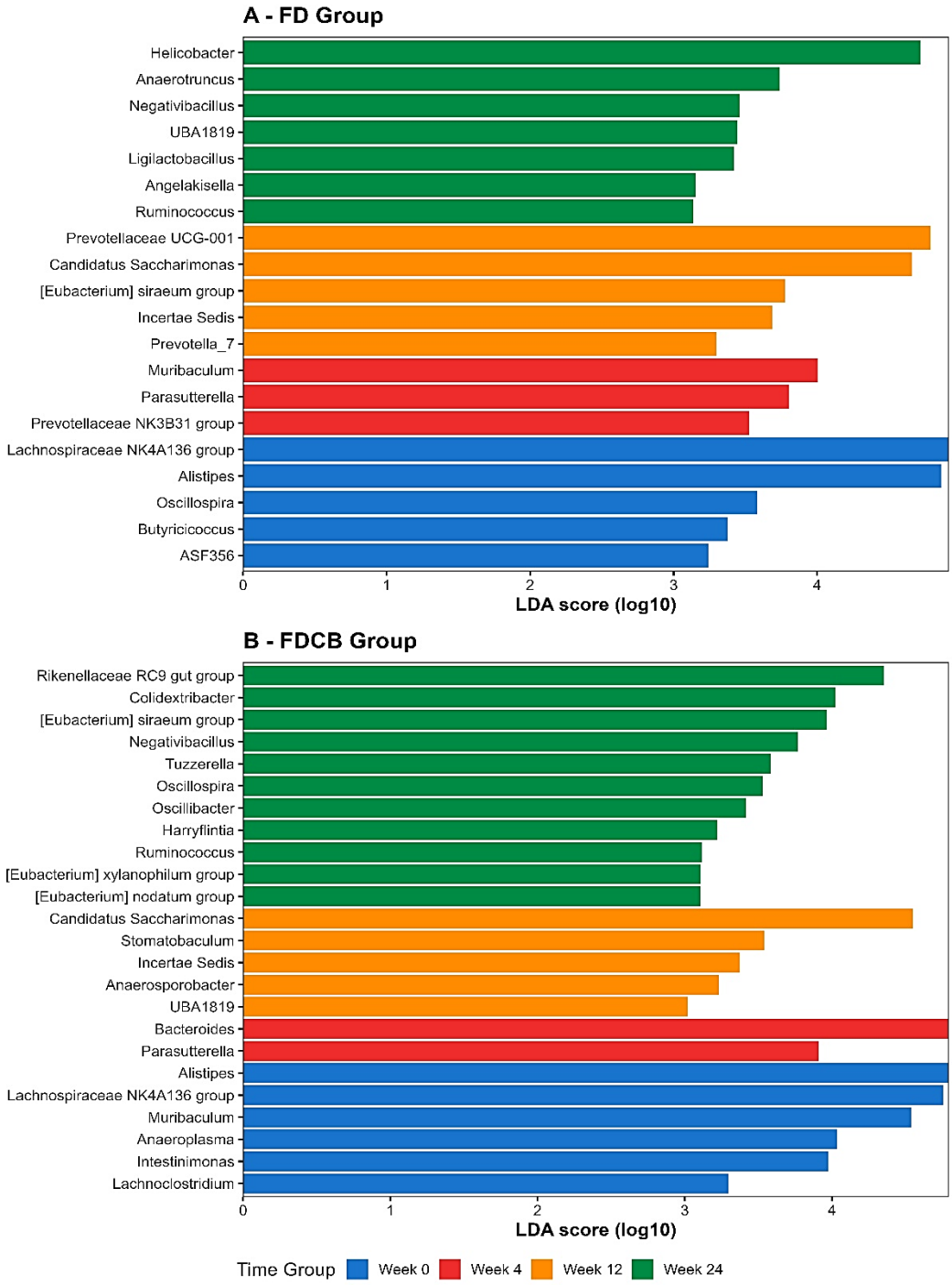

Figure 5. LEfSe (Linear Discriminant Analysis Effect Size) was applied to identify bacterial genera significantly enriched in each diet group (FD and FDCB) across all time points (Weeks 0, 4, 12 and 24). The bar plots show taxa with an LDA score >3 and p-value <0.05. Panel **A** represents genera enriched in the FD group and Panel **B** in the FDCB group.

3.4 METABOLIC STATUS AND IMMUNE CELL POPULATIONS PROFILING IN VISCERAL ADIPOSE TISSUE

Metabolic profiling at week 24 revealed that most serum parameters did not differ significantly between FD and FDCB fed mice (Figure 6). Glucose tended to be lower in FDCB animals, but this drop did not reach significance. Cholesterol was unchanged; triglycerides showed a modest increase under FDCB, total proteins and albumin were also comparable. Liver enzymes AST and ALT showed no diet related elevations. In contrast, the two adipokines measured diverged markedly: Leptin was substantially lower in FDCB fed mice and Adiponectin was significantly higher in this group.

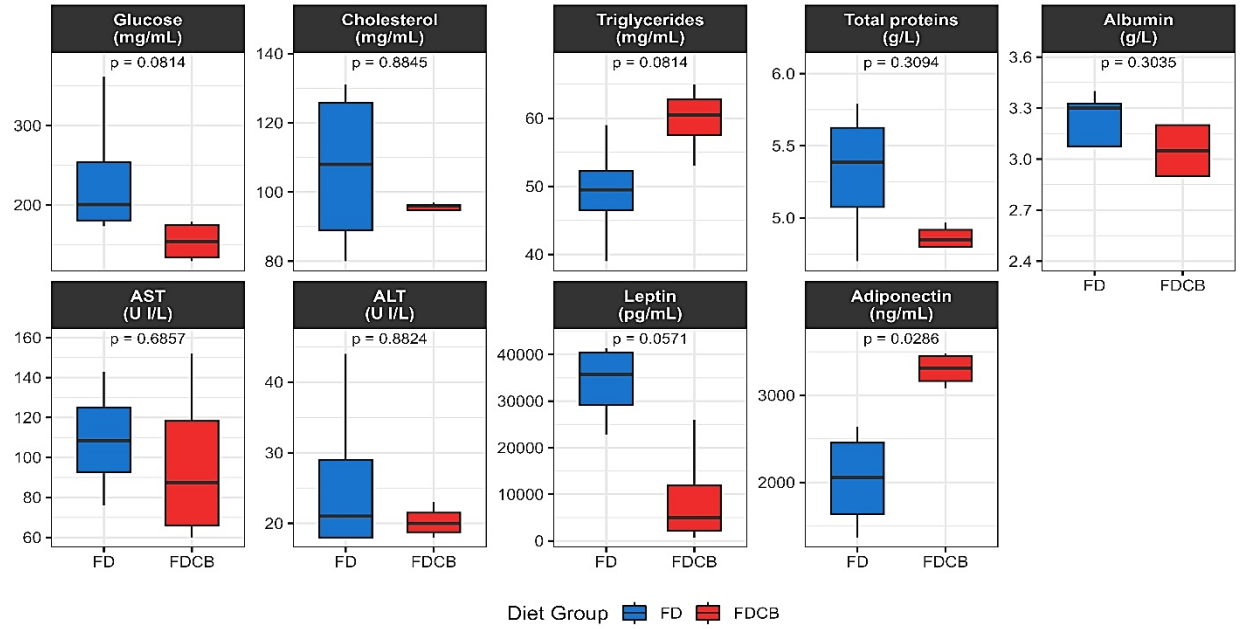

Figure 6. Boxplots showing circulating levels of glucose, cholesterol, triglycerides, total proteins, albumin, AST, ALT, leptin and adiponectin in mice fed FD (blue) or a FDCB (red) after 24 weeks of intervention.

Immune phenotyping of VAT at week 24 demonstrated diet-specific shifts in Tregs markers, whereas the myeloid cell subsets remained largely unaffected (Figure 7). The overall frequency of $CD4^+$ T cells (% $CD45^+$ $CD4^+$) was lower in FDCB-fed mice compared with FD controls, but this did not reach statistical significance. In contrast, the proportion of $FOXP3^+$ Tregs (% $CD45^+$ $CD4^+$ $FOXP3^+$) was markedly reduced by FDCB feeding, while the fraction of IL-10–producing Tregs (% $CD45^+$ $CD4^+$ $FOXP3^+$ IL-10^+) trended lower in FDCB mice, but this difference was not significant. Strikingly, the per cell expression of IL-10 (MFI) in the $FOXP3^+$ subset was substantially higher under FDCB versus FD, indicating that although lower in number, FDCB Tregs produce more IL-10 per cell. By contrast, markers of the myeloid lineage and F4/80+ macrophages were unaffected.

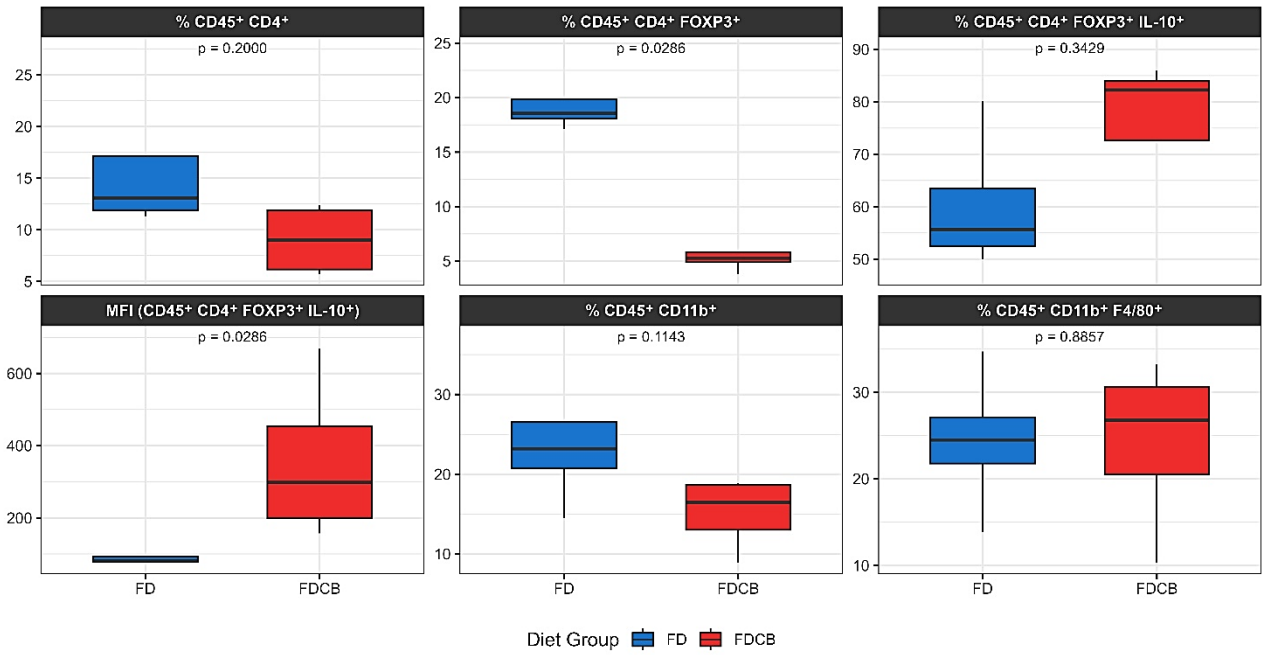

Figure 7. Boxplots representing proportions and Median fluorescence intensity (MFI) of specific immune cell subsets in mice fed a high-fat diet (FD, blue) or a high-fat diet supplemented with choline and betaine (FDCB, red) after 24 weeks. Evaluated markers include total $CD4^+$ T cells, Tregs ($CD4^+$ $FOXP3^+$), IL-10^+ Tregs, myeloid and macrophages cell populations ($CD11b^+$, $CD11b^+$ F4/80^+) and MFI of IL-10^+ Tregs.

To further characterize the Tregs compartment, we calculated multiple functional indices integrating IL-10 expression, Treg frequency and CD4⁺ T cell context (Figure 8). Despite the overall reduction in FOXP3⁺ Treg frequency under FDCB feeding, the proportion of IL-10⁺ Tregs relative to total Tregs was markedly higher in this group. Similarly, the MFI (IL-10) normalized to IL-10⁺ Tregs was significantly elevated, reinforcing the notion that FDCB enhances Treg suppressive potential.

The overall Tregs/CD4⁺ ratio was lower in FDCB-fed animals, but this difference was not statistically significant. In contrast, the ratio of IL-10⁺ Tregs to total CD4⁺ T cells showed a strong trend toward enrichment under FDCB.

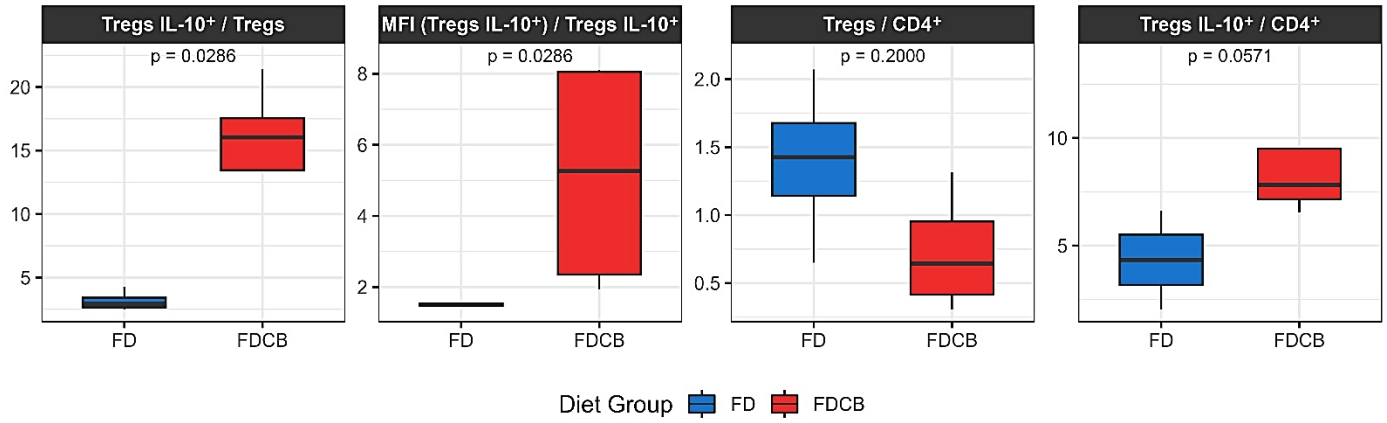

Figure 8. Boxplots represent the proportions and fluorescence based ratios of IL-10⁺ Tregs in mice fed a FD (blue) or a FDCB (red) at week 24. Shown are: the percentage of IL-10⁺ Tregs among total Tregs, IL-10 median fluorescence intensity (MFI) per IL-10⁺ Treg, Treg/CD4⁺ ratio and IL-10⁺ Tregs per CD4⁺ T cells.

3.5 CORRELATION BETWEEN GUT MICROBIOTA COMPOSITION AND BODY WEIGHT

The relationship between animal body weight and the relative abundance of bacterial genera is presented in Figure 9. A subset of taxa showed statistically significant associations ($p < 0.05$, green dots), with notable positive correlations observed for genera such as *Ligilactobacillus*, *[Eubacterium] nodatum group*, *Faecalibacterium*, *Roseburia*, and *[Ruminococcus] gnavus group*, among others. These microorganisms were associated with increased body weight. Conversely, significant negative correlations were observed for genera such as *Alistipes*, *ASF356*, *Muribaculum*, *Butyricicoccus* and *Anaeroplasma*, whose lower abundance was related to higher body weight.

3.5.1 Integrative immuno-metabolic and microbiota analysis using DIABLO multiblock framework

To explore coordinated responses across microbiota composition, immune profiles in VAT and systemic metabolic parameters, we applied a DIABLO integrative multiblock analysis. The model robustly discriminated mice according to diet (FD vs. FDCB), achieving clear group separation across all three data blocks: microbiota, immunity and metabolism (Supplementary Figure S1).

Variable loading plots revealed that the genera *Harryflintia, Lachnospiraceae UCG-009, Oscillibacter, Oscillospira* and *Flavonifractor* contributed most strongly to the microbiota signature of FDCB fed mice. In contrast, *Helicobacter* was uniquely enriched in FD animals considering Component 1 (Supplementary Figure S2 A-B). Immune variables that drove separation included elevated IL-10 expression on Tregs (Tregs IL-10⁺/Tregs and MFI (Tregs IL10⁺) in FDCB mice, whereas the overall Tregs percentage was higher in the FD group (Supplementary Figure S2 C-D). On the metabolic axis, FDCB mice were associated with higher adiponectin and triglycerides, while FD mice showed higher leptin, glucose and total protein levels (Supplementary Figure S2 E-F).

A circus plot summarizing cross-domain correlations (cut-off |r| > 0.7) revealed that *Flavonifractor, Oscillibacter*, *Lachnospiraceae UCG-009* and *Harryflintia* positively correlated with IL-10-producing Tregs and adiponectin levels (Figure 10A). Notably, leptin levels inversely correlated with Treg IL-10 indices and beneficial taxa enriched under FDCB, suggesting immuno-metabolic remodeling driven by the diet.

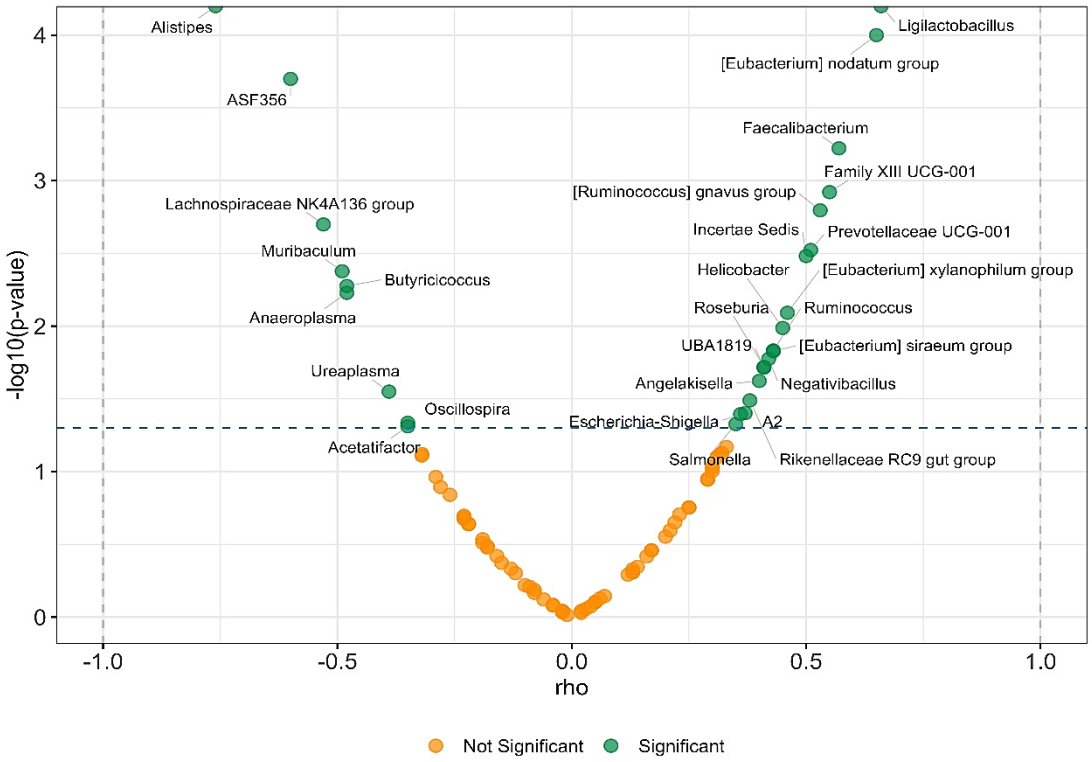

Figure 9. Spearman correlation analysis between the relative abundance of bacterial genera and body weight across all samples. Each point represents a genus, plotted according to its Spearman rho coefficient (x-axis) and the statistical significance ($-\log_{10}$ p-value; y-axis). Genera with significant correlations ($p < 0.05$) are highlighted in green, while non-significant correlations are shown in orange. Positive correlations are located on the right and negative correlations on the left.

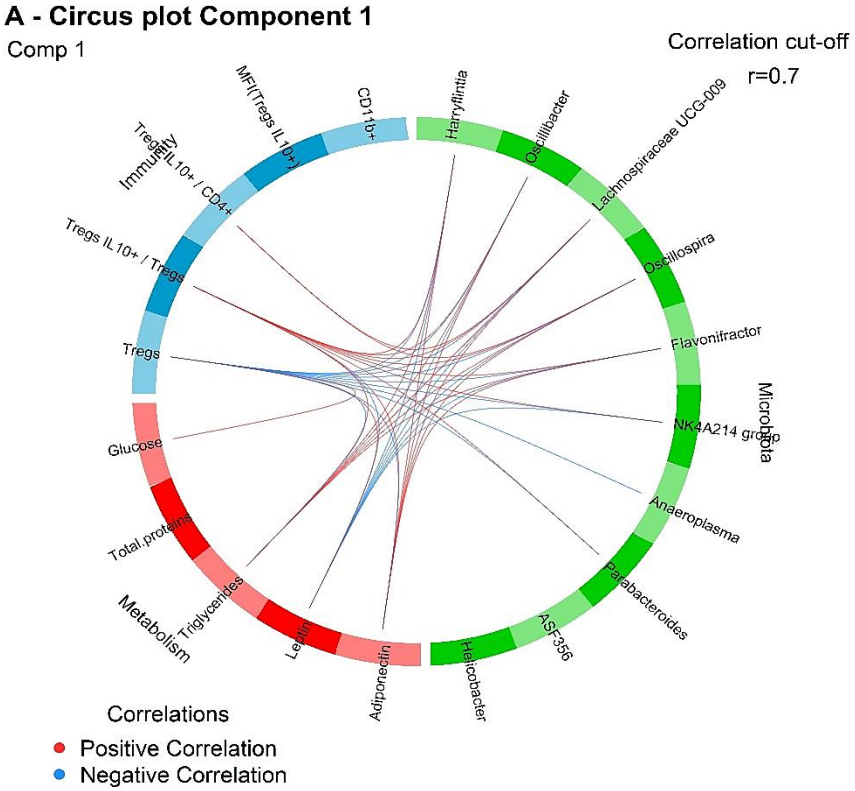

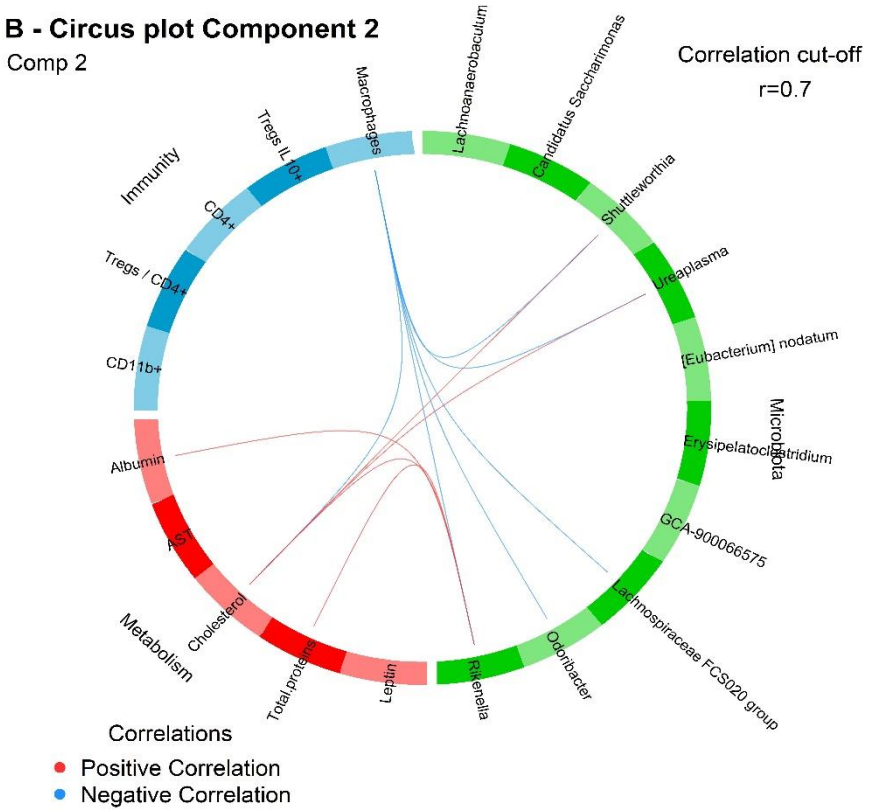

Figure 10. Circus plots from the multiblock DIABLO analysis showing correlations (|r| > 0.7) among discriminant variables from microbiota (green), metabolic (red) and immune (blue) blocks. **(A)** Component 1; **(B)** Component 2. Red ribbons indicate positive correlations, while blue ribbons indicate negative correlations. Only variables with high contributions to group separation are included.

Discussion

Our findings demonstrate that dietary supplementation with choline and betaine exerts beneficial, multi-layered effects in a mouse model of DIO, including delayed weight gain, modulation of gut microbiota composition, improved adipokine profiles and the emergence of anti-inflammatory immune signatures in VAT. This exploratory study supports the growing notion that methyl-donor nutrients can influence host immunometabolic homeostasis by acting through the gut–VAT–immune axis.

FDCB fed mice exhibited significantly reduced body weight gain across the 24-week period, despite similar caloric intake to FD fed controls, highlighting a marked delay in obesity onset associated with choline and betaine supplementation. This observation aligns with previous reports suggesting that choline and betaine modulate energy metabolism through epigenetic regulation of genes involved in lipid handling, insulin sensitivity and adipogenesis such as PPARγ and FASN[31–34]. Beyond body weight, FDCB fed mice showed lower serum leptin and higher adiponectin levels, consistent with improved adipocyte function and systemic metabolic tone[35].

Another key anti-inflammatory mechanism induced by choline/betaine is elevation of IL-10, an anti-inflammatory cytokine closely tied to regulatory immune responses in VAT. While IL-10 is not an adipokine per se, its production by immune cells in adipose tissue and gut is enhanced indirectly via the microbiota and metabolite changes brought by choline and betaine. In DIO mice, improved metabolic status often correlates with higher production of IL-10, reflecting a reduction in systemic inflammation and suggesting remodeling of immune regulation toward fewer but functionally enhanced Tregs. This can be partly attributed to SCFAs produced by gut microbes (see below); these metabolites stimulate differentiation of Tregs which secrete IL-10, thereby

buffering obesity-related inflammation[30]. Butyrate, for instance, has been shown to upregulate FOXP3 in Tregs and drive IL-10 production, while concurrently suppressing pro inflammatory Th17 cells[36–38].

Therefore, by promoting a gut environment rich in SCFAs (through microbiota changes), choline and betaine supplementation can increase IL-10 and other anti-inflammatory mediators. Indeed, experimental evidence suggests that SCFAs and their downstream signals (e.g. GPR41/43 receptors and HDAC inhibition) induce Tregs and IL-10, contributing to reduced adipose and systemic inflammation[39].

Microbiota analysis in samples taken 24 weeks post diet revealed that FDCB feeding led to the enrichment of genera with known SCFA producing or immunomodulatory capacities, these includes *Parabacteroides, Oscillospira, Flavonifractor, Harryflintia,* and *Christensenellaceae R7 group*. Besides, these taxa have been associated with metabolic flexibility, mucosal integrity and lean phenotypes in both preclinical and human studies [40–43]. Moreover, *Parabacteroides* and *Alistipes* genera have consistently been associated with reduced adiposity, lean phenotypes, anti-inflammatory properties, increased mucin production and enhanced intestinal barrier function supporting that the FDCB diet fosters a gut microbial environment conducive to metabolic resilience[44,45]. Conversely, genera enriched in the FD group (*Helicobacter, Negativibacillus*) have been linked to pro-inflammatory phenotypes and adverse metabolic profiles[46,47].

The systems level implications of these shifts were captured using a multiblock integrative approach. The DIABLO model robustly discriminated mice by diet across gut microbiota, immune and metabolic domains. Taxa enriched in FDCB fed group (*Flavonifractor, Lachnospiraceae UCG-009, Oscillibacter, Oscillospira, Harryflintia*) showed strong positive correlations with IL-10 producing Tregs and adiponectin levels, key hallmarks of anti-inflammatory and metabolically protective states.

This integrative analysis underscores that choline and betaine supplementation does not exert isolated effects, but rather orchestrates a coordinated remodeling of host–microbe interactions that spans immune and metabolic compartments. The ability of DIABLO to identify key cross-domain drivers highlights the potential of using gut microbial features as biomarkers of dietary response or targets for precision nutrition strategies.

Importantly, while our findings support the therapeutic potential of choline and betaine, caution is warranted due to the possible production of trimethylamine (TMA) and its pro-atherogenic derivative, trimethylamine N-oxide (TMAO). The production of TMA from choline depends on microbiota composition and is driven by specific taxa such as *Clostridia, Desulfovibrio and Enterobacteriaceae*[48,49]. In contrast, certain *Bacteroides* species may limit TMA generation. Thus, the cardiometabolic safety of choline/betaine supplementation may require individual microbiota profiling or co-interventions (e.g., TMA-lyase inhibitors or SCFA-enhancing probiotics) to minimize TMAO related risks[50].

Our findings are consistent with recent clinical observations. A 2024 population-based study in China reported that individuals in the highest quartile of dietary betaine intake had significantly lower BMI, reduced hip circumference and decreased obesity prevalence[51] .

Furthermore, ongoing clinical trials (e.g., NCT06758856) are exploring the impact of choline-betaine supplementation on microbiota and metabolic outcomes in overweight adults, underscoring the translational relevance of our findings.

Beyond serving as a mediator of downstream metabolic and immune effects, the gut microbiota emerges in this study as a central hub through which choline and betaine exert their systemic influence. The distinct microbial signatures observed in FDCB fed mice, particularly the enrichment of SCFA-producing and immunoregulatory taxa, suggest that modulation of microbial community structure is not merely a consequence but a key mechanism of dietary intervention. These microbial changes may precede or even initiate host immunometabolic

remodeling, positioning the microbiota as a therapeutic target in itself. Future mechanistic studies employing microbiota transfer or gnotobiotic models will be essential to unravel causality and identify specific microbial consortia or metabolites responsible for the observed effects. Moreover, the predictive value of microbial profiles uncovered through DIABLO integration reinforces the relevance of microbiota-based biomarkers for stratifying dietary responders and guiding precision nutritional interventions in obesity management.

While our results highlight biologically meaningful shifts in gut microbial composition, driving immune regulation in VAT and metabolic outcomes, it is important to acknowledge that this is an exploratory pilot study with a small sample size. Nevertheless, the consistency of the trends observed across multiple biological layers adds robustness to the integrative model and supports the rationale for conducting larger scale, longitudinal studies to validate and expand upon these observations.

5. Conclusion

In conclusion, the FDCB diet promotes a favorable shift in gut microbial ecology, enriches immune-regulatory taxa and enhances systemic metabolic parameters, notably through the expansion of SCFA producers and IL-10 associated Tregs. The use of DIABLO modeling reveals coherent microbiota–immune–metabolism interactions that may underpin these effects and supports the rationale for microbiota informed dietary interventions. Given the exploratory nature of this study and the limited number of animals per group, these results should be considered hypothesis generating. Larger, powered studies will be essential to confirm these findings and determine their translational relevance.

Supplementary Materials:

Supplementary Table S1A: Supplementary Table S1A: Body weight analysis; Supplementary Table S2: Alpha diversity analysis; S3: Beta diversity analysis; Supplementary Table S4: Blood metabolic parameters analysis; Supplementary Table S4: Differential bacterial taxa identified by LEfSe analysis across dietary groups at different time points. Supplementary Table S5: Differential bacterial genera identified by LEfSe analysis across time points in response to dietary interventions. Supplementary Table S6. Circulating metabolic parameters in mice after 24 weeks of dietary intervention. Supplementary Table S7. Immune cell populations in the stromal vascular fraction of visceral adipose tissue after 24 weeks of dietary intervention. Supplementary Table S8. Correlation between bacterial genera and body weight. Supplementary Figure S1. Discrimination of diet groups across data blocks in DIABLO analysis. Supplementary Figure S2. Variable contributions from each data block (microbiota, immunity, and metabolism) to the DIABLO integrative model components.

Supplementary Table S1: Body weight analysis

Week	FD (Median [IQR], g)	FDCB (Median [IQR], g)	p-value
Week 0	26.4 (24.5–28.5)	25.2 (24.9–26.0)	0.8860
Week 4	35.3 (33.8–37.0)	30.1 (29.0–31.0)	**0.0294**
Week 12	38.4 (36.4–40.3)	32.9 (31.5–34.0)	**0.0286**
Week 24	44.7 (44.2–45.5)	38.0 (36.8–39.2)	**0.0294**

Supplementary Table S1. *Body weight analysis at weeks 0, 4, 12, and 24 in mice subjected to different dietary interventions (FD vs. FDCB). Values are presented as median and interquartile range (IQR). Statistical comparisons between groups were performed using the Wilcoxon rank-sum test. p-values in bold indicate statistically significant differences ($p < 0.05$).*

Abbreviations: *FD: high-fat diet; FDCB: high-fat diet supplemented with choline and betaine.*

Supplementary Table S2: Alpha diversity analysis

Week	Metric	FD (median [IQR])	FDCB (median [IQR])	p-value
Week 0	Observed	865.5 (853.8–878.8)	832.5 (827.5–842.2)	0.1124
Week 0	Chao1	946.9 (927.9–970.1)	927.3 (917.2–939.5)	0.4705
Week 0	Shannon	5.7 (5.7–5.7)	5.5 (5.5–5.5)	**0.0304**
Week 0	Simpson	1.0 (1.0–1.0)	1.0 (1.0–1.0)	**0.0304**
Week 4	Observed	832.5 (768.8–902.5)	925.0 (885.0–946.2)	0.4705
Week 4	Chao1	922.8 (854.0–998.1)	1033.6 (994.7–1051.5)	0.4705
Week 4	Shannon	5.4 (5.3–5.5)	5.7 (5.6–5.7)	**0.0606**
Week 4	Simpson	1.0 (1.0–1.0)	1.0 (1.0–1.0)	**0.0304**
Week 12	Observed	863.5 (825.5–903.0)	952.5 (932.8–966.2)	0.1124
Week 12	Chao1	934.1 (906.4–986.1)	1039.1 (1027.1–1054.5)	0.1939
Week 12	Shannon	5.4 (5.4–5.5)	5.7 (5.7–5.7)	**0.0304**
Week 12	Simpson	1.0 (1.0–1.0)	1.0 (1.0–1.0)	**0.0304**
Week 24	Observed	841.5 (792.0–876.2)	987.5 (947.5–1000.8)	0.1124
Week 24	Chao1	938.6 (887.3–969.9)	1072.8 (1040.0–1088.2)	0.1124
Week 24	Shannon	5.3 (5.2–5.4)	5.8 (5.7–5.8)	0.0606
Week 24	Simpson	1.0 (1.0–1.0)	1.0 (1.0–1.0)	0.0606

Supplementary Table S2. *Alpha diversity analysis at weeks 0, 4, 12, and 24 in mice subjected to different dietary interventions (FD vs. FDCB). Values are presented as median and interquartile range (IQR). Alpha diversity was assessed using four metrics: Observed species richness, Chao1 estimator, Shannon index, and Simpson index. Statistical comparisons between groups were performed using the Wilcoxon rank-sum test. p-values in bold indicate statistically significant differences ($p < 0.05$).*

Supplementary Table S3: Beta diversity analysis

Week	Method	R	p-value
Week 0	Unweighted UniFrac	0.8438	**0.022**
Week 0	Weighted UniFrac	-0.0104	0.341
Week 4	Unweighted UniFrac	0.9583	0.036
Week 4	Weighted UniFrac	-0.4896	1
Week 12	Unweighted UniFrac	0.4583	0.060
Week 12	Weighted UniFrac	-0.0625	0.684
Week 24	Unweighted UniFrac	0.8958	**0.031**
Week 24	Weighted UniFrac	0.125	**0.035**

Supplementary Table S3. *Analysis of group differences in beta diversity across time points (Weeks 0, 4, 12, and 24) using ANOSIM (Analysis of Similarities) based on unweighted and weighted UniFrac distances.*

The R statistic indicates the degree of separation between groups, where values closer to 1 reflect stronger dissimilarity. p-values indicate statistical significance; values in bold represent significant differences ($p < 0.05$).

Abbreviations: R*: ANOSIM statistic;* p*: p-value from 999 permutations.*

Supplementary Table S4: Differential bacterial taxa identified by LEfSe analysis across dietary groups at different time points.

Week	Taxon	Enriched Group	LDA Score (log10)	p-value
Week 0	Tuzzerella	FD	3.68	0.0209
Week 0	[Eubacterium] xylanophilum group	FD	3.27	0.0209
Week 0	Herbinix	FD	3.11	0.0433
Week 0	Anaerostipes	FD	3.02	0.0421
Week 0	Muribaculum	FDCB	4.74	0.0209
Week 0	Intestinimonas	FDCB	4.24	0.0209
Week 0	Parabacteroides	FDCB	3.92	0.0433
Week 0	Prevotella_7	FDCB	3.47	0.0209
Week 0	UCG-009	FDCB	3.24	0.0433
Week 4	Helicobacter	FD	4.74	0.0433
Week 4	Lachnoanaerobaculum	FD	4.5	0.0209
Week 4	Lachnospiraceae UCG-001	FD	3.8	0.0433
Week 4	UCG-001	FD	3.71	0.0209
Week 4	Tuzzerella	FD	3.51	0.0209
Week 4	[Eubacterium] xylanophilum group	FD	3.44	0.0209
Week 4	Parabacteroides	FDCB	4.47	0.0209
Week 4	ASF356	FDCB	3.64	0.018
Week 4	Stomatobaculum	FDCB	3.22	0.0421
Week 4	Ruminococcus	FDCB	3.17	0.0421
Week 4	Christensenellaceae R-7 group	FDCB	3.17	0.0139
Week 4	Paludicola	FDCB	3.06	0.0202
Week 12	Stomatobaculum	FD	3.71	0.0209
Week 12	Negativibacillus	FD	3.7	0.0209
Week 12	ASF356	FD	3.49	0.0433
Week 12	Anaerosporobacter	FD	3.38	0.0209
Week 12	Anaerovorax	FD	3.22	0.0209
Week 12	Harryflintia	FD	3.2	0.0433
Week 24	Helicobacter	FD	4.95	0.0209
Week 24	Lachnoanaerobaculum	FD	4.53	0.0433
Week 24	Parasutterella	FD	3.9	0.0209
Week 24	Anaerotruncus	FD	3.76	0.0433
Week 24	Flavonifractor	FDCB	4.1	0.0209
Week 24	Parabacteroides	FDCB	4.09	0.0209
Week 24	Oscillospira	FDCB	3.87	0.0209
Week 24	Oscillibacter	FDCB	3.83	0.0209
Week 24	Harryflintia	FDCB	3.39	0.0209
Week 24	Christensenellaceae R-7 group	FDCB	3.28	0.0202

Supplementary Table S4. *Significantly enriched bacterial genera identified by LEfSe analysis (LDA >3, p <0.05) in mice under different dietary interventions (FD vs. FDCB) at weeks 0, 4, 12, and 24. The table shows the name of the taxon, the diet group in which it was enriched, the LDA effect size (log10 scale), and the p-value.*

Abbreviations: FD: *high-fat diet; FDCB: high-fat diet supplemented with choline and betaine.*

Supplementary Table S5: Differential bacterial genera identified by LEfSe analysis across time points in response to dietary interventions.

Diet	Feature	Enriched Group	LDA Score (log10)	p-value
FD	Lachnospiraceae NK4A136 group	Week 0	4.92	0.0482
FD	Alistipes	Week 0	4.86	0.0198
FD	Oscillospira	Week 0	3.58	0.0361
FD	Butyricicoccus	Week 0	3.38	0.0305
FD	ASF356	Week 0	3.24	0.0440
FD	Muribaculum	Week 4	4.00	0.0415
FD	Parasutterella	Week 4	3.80	0.0450
FD	Prevotellaceae NK3B31 group	Week 4	3.53	0.0275
FD	Prevotellaceae UCG-001	Week 12	4.79	0.0330
FD	Candidatus Saccharimonas	Week 12	4.66	0.0115
FD	[Eubacterium] siraeum group	Week 12	3.78	0.0088
FD	Incertae Sedis	Week 12	3.69	0.0122
FD	Prevotella_7	Week 12	3.30	0.0351
FD	Helicobacter	Week 24	4.72	0.0454
FD	Anaerotruncus	Week 24	3.74	0.0168
FD	Negativibacillus	Week 24	3.46	0.0165
FD	UBA1819	Week 24	3.44	0.0287
FD	Ligilactobacillus	Week 24	3.42	0.0198
FD	Angelakisella	Week 24	3.15	0.0257
FD	Ruminococcus	Week 24	3.14	0.0085
FDCB	Alistipes	Week 0	4.79	0.0101
FDCB	Lachnospiraceae NK4A136 group	Week 0	4.75	0.0361
FDCB	Muribaculum	Week 0	4.54	0.0053
FDCB	Anaeroplasma	Week 0	4.03	0.0334
FDCB	Intestinimonas	Week 0	3.98	0.0252
FDCB	Lachnoclostridium	Week 0	3.30	0.0057
FDCB	Bacteroides	Week 4	4.79	0.0492
FDCB	Parasutterella	Week 4	3.91	0.0202
FDCB	Candidatus Saccharimonas	Week 12	4.55	0.0369
FDCB	Stomatobaculum	Week 12	3.54	0.0415
FDCB	Incertae Sedis	Week 12	3.37	0.0252
FDCB	Anaerosporobacter	Week 12	3.23	0.0110
FDCB	UBA1819	Week 12	3.02	0.0048
FDCB	Rikenellaceae RC9 gut group	Week 24	4.35	0.0334
FDCB	Colidextribacter	Week 24	4.02	0.0305
FDCB	[Eubacterium] siraeum group	Week 24	3.97	0.0061
FDCB	Negativibacillus	Week 24	3.77	0.0101
FDCB	Tuzzerella	Week 24	3.59	0.0314
FDCB	Oscillospira	Week 24	3.53	0.0281
FDCB	Oscillibacter	Week 24	3.42	0.0459
FDCB	Harryflintia	Week 24	3.22	0.0217
FDCB	Ruminococcus	Week 24	3.12	0.0348
FDCB	[Eubacterium] xylanophilum group	Week 24	3.11	0.0202
FDCB	[Eubacterium] nodatum group	Week 24	3.11	0.0196

Supplementary Table S5. *Significantly enriched bacterial genera identified by LEfSe analysis (LDA >3, p <0.05) across all time points for each dietary group (FD vs. FDCB). The table presents the genus name, the specific time point at which it was enriched, the LDA effect size (log10 scale), and the corresponding p-value. This integrative analysis highlights consistent microbial signatures associated with each dietary intervention throughout the experimental period.*

Abbreviations: *FD: high-fat diet; FDCB: high-fat diet supplemented with choline and betaine.*

Supplementary Table S6. Circulating metabolic parameters in mice after 24 weeks of dietary intervention.

Metabolic Parameter	FD (median [IQR])	FDCB (median [IQR])	p-value
Glucose (mg/dL)	201(181–254)	154.0 (133.5–174.5)	0.0814
Cholesterol (mg/dL)	108 (89–126)	96 (95–96)	0.8845
Triglycerides (mg/dL)	49.5 (46.5–52.2)	61 (58–63)	0.0814
Total proteins (g/L)	5.4 (5.1–5.6)	4.8 (4.8–4.9)	0.3094
Albumin (g/L)	3.3 (3.1–3.3)	3.0 (2.9–3.2)	0.3035
AST (UI/L)	109 (93–125)	88 (66–118)	0.6857
ALT (UI/L)	21 (18–29)	20.0 (18.8–21.5)	0.8824
Leptin (pg/mL)	35713 (29196–40434)	4942 (2213–11871)	0.0571
Adiponectin (ng/mL)	2058 (1635–2455)	3314 (3164–3447)	0.0286

Supplementary Table S6. *Concentrations of metabolic markers in plasma from mice under FD or FDCB diets. The table includes values for glucose, cholesterol, triglycerides, total proteins, albumin, AST, ALT, leptin, and adiponectin. Data are presented as median and interquartile range (IQR). Statistical differences between groups were assessed using the Wilcoxon rank-sum test, with associated p-values reported.*

Abbreviations: *FD: high-fat diet; FDCB: high-fat diet supplemented with choline and betaine.*

Supplementary Table S7. Immune cell populations in the stromal vascular fraction of visceral adipose tissue after 24 weeks of dietary intervention.

Cytometry Parameter in Visceral Adipose Tissue	FD (median [IQR])	FDCB (median [IQR])	p-value
% $CD45^+$ $CD4^+$	13.1 (11.9–17.1)	9.0 (6.2–11.9)	0.2000
% $CD45^+$ $CD4^+$ $FOXP3^+$ (Tregs)	18.5 (18.1–19.9)	5.3 (4.9–5.8)	0.0286
% $CD45^+$ $CD4^+$ $FOXP3^+$ $IL10^+$	55.6 (52.5–63.5)	82.2 (72.7–84.0)	0.3429
MFI ($CD45^+$ $CD4^+$ $FOXP3^+$ $IL10^+$)	81.2 (78.2–92.9)	298.0 (199.8–453.8)	0.0286
% $CD45^+$ $CD11b^+$	23.2 (20.7–26.6)	16.5 (13.0–18.7)	0.1143
% $CD45^+$ $CD11b^+$ $F4/80^+$	24.5 (21.8–27.1)	26.8 (20.5–30.6)	0.8857
Ratio (Tregs $IL10^+$ / Tregs)	2.9 (2.7–3.4)	16.0 (13.4–17.5)	0.0286
Ratio (MFI(Tregs $IL10^+$) / Tregs $IL10^+$)	1.5 (1.5–1.5)	5.3 (2.3–8.1)	0.0286
Ratio (Tregs / $CD4^+$)	1.4 (1.1–1.7)	0.6 (0.4–1.0)	0.2000
Ratio (Tregs $IL10^+$ / $CD4^+$)	4.3 (3.2–5.5)	7.8 (7.1–9.5)	0.0571

Supplementary Table S7. *Quantification of immune cell subsets isolated from the stromal vascular fraction of visceral adipose tissue in mice fed FD or FDCB diets. The table presents values for the percentage of $CD45^+$ $CD4^+$ T cells, $CD4^+$ $FOXP3^+$ regulatory T cells, and IL-10^+ subsets, as well as myeloid cells expressing CD11b and F4/80. Additionally, it includes the median fluorescence intensity (MFI) of IL-10 in Tregs and several calculated ratios: IL-10^+ Tregs over total Tregs, MFI of IL-10^+ Tregs over IL-10^+ Tregs, total Tregs over $CD4^+$ T cells, and IL-10^+ Tregs over $CD4^+$ T cells. Data are expressed as medians with interquartile ranges (IQR). P-values were obtained using Wilcoxon rank-sum tests.*

Abbreviations: FD: *high-fat diet; FDCB: high-fat diet supplemented with choline and betaine; MFI: median fluorescence intensity; CD: cluster of differentiation.*

Supplementary Table S8. Correlation between bacterial genera and body weight.

Genus	rho	p-value
Alloprevotella	0.13	0.4696
Prevotellaceae UCG-001	0.51	0.0030
Lachnoanaerobaculum	0.31	0.0800
Helicobacter	0.45	0.0103
Rikenellaceae RC9 gut group	0.38	0.0324
Candidatus Saccharimonas	0.30	0.0989
Flavonifractor	-0.19	0.3088
Colidextribacter	0.02	0.9347
Parasutterella	-0.18	0.3337
Bacteroides	0.32	0.0745
Odoribacter	-0.32	0.0776
Intestinimonas	-0.15	0.4234
Oscillospira	-0.35	0.0462
Muribaculum	-0.49	0.0042
Herbinix	0.29	0.1138
Negativibacillus	0.42	0.0168
Parabacteroides	-0.29	0.1088
Alistipes	-0.76	<0.0001
[Ruminococcus] gnavus group	0.53	0.0016
Oscillibacter	-0.18	0.3259
Ligilactobacillus	0.66	<0.0001
Lachnospiraceae NK4A136 group	-0.53	0.0020
Anaerotruncus	0.04	0.8434
[Eubacterium] xylanophilum group	0.46	0.0081
Prevotella_7	-0.02	0.9071
Harryflintia	0.22	0.2236
Desulfovibrio	0.16	0.3824
Tuzzerella	0.17	0.3482
Anaeroplasma	-0.48	0.0059
UCG-009	0.03	0.8789
Mucispirillum	0.12	0.5102
UCG-001	0.13	0.4931
Incertae Sedis	0.5	0.0033
Butyricicoccus	-0.48	0.0053
Rikenella	-0.08	0.6804
Stomatobaculum	-0.06	0.7557
Prevotellaceae NK3B31 group	0.29	0.1118
Lactobacillus	-0.28	0.1276
[Eubacterium] eligens group	0.32	0.0751
GCA-900066575	-0.23	0.2012
[Eubacterium] siraeum group	0.43	0.0149
Ruminococcus	0.43	0.0147
Acetatifactor	-0.35	0.0488
HT002	-0.16	0.3805
Angelakisella	0.4	0.0238
Lachnospiraceae UCG-006	-0.02	0.9281

ASF356	-0.6	0.0002
[Eubacterium] nodatum group	0.65	0.0001
UCG-003	-0.1	0.6023
Roseburia	0.41	0.0191
Erysipelatoclostridium	0.2	0.2800
Bilophila	-0.08	0.6489
UBA1819	0.41	0.0193
Paludicola	-0.01	0.9666
Anaerosporobacter	-0.13	0.4640
Escherichia-Shigella	0.36	0.0403
UCG-002	-0.04	0.8234
Shuttleworthia	0.02	0.9068
V9D2013 group	-0.04	0.8335
NK4A214 group	0.13	0.4910
Anaerovorax	0.05	0.7915
A2	0.37	0.0396
Lachnoclostridium	-0.12	0.4991
Lachnospiraceae UCG-003	0.05	0.7865
Ureaplasma	-0.39	0.0282
Christensenellaceae R-7 group	-0.09	0.6198
Anaerostipes	0.3	0.0918
Peptococcus	0.31	0.0791
Mobilitalea	0.07	0.7165
Akkermansia	-0.22	0.2288
[Eubacterium] fissicatena group	0.25	0.1765
Lachnospiraceae UCG-001	0.23	0.1968
Tyzzerella	-0.02	0.9092
Dubosiella	-0.23	0.2118
Lachnospiraceae UCG-009	-0.19	0.2919
Monoglobus	0.33	0.0677
Family XIII UCG-001	0.55	0.0012
Family XIII AD3011 group	0.21	0.2533
Marvinbryantia	-0.32	0.0756
Salmonella	0.35	0.0472
Lactococcus	0.25	0.1763
Lachnospiraceae UCG-004	-0.22	0.2301
Merdibacter	0.17	0.3475
UC5-1-2E3	0.06	0.7437
Lachnospiraceae FCS020 group	0.14	0.4513
Olsenella	0.3	0.0940
Mycoplasma	-0.26	0.1444
Lachnospiraceae AC2044 group	-0.23	0.2063
Faecalibacterium	0.57	0.0006

Supplementary Table S8. *The table presents the results of Spearman correlation analyses between the relative abundance of bacterial genera and body weight in all experimental samples. For each genus, the table reports the correlation coefficient (rho)and the associated p-value.*

Abbreviations: rho: *Spearman correlation coefficient; p-value: statistical significance.*

Supplementary Figure S1. Discrimination of diet groups across data blocks in DIABLO analysis.

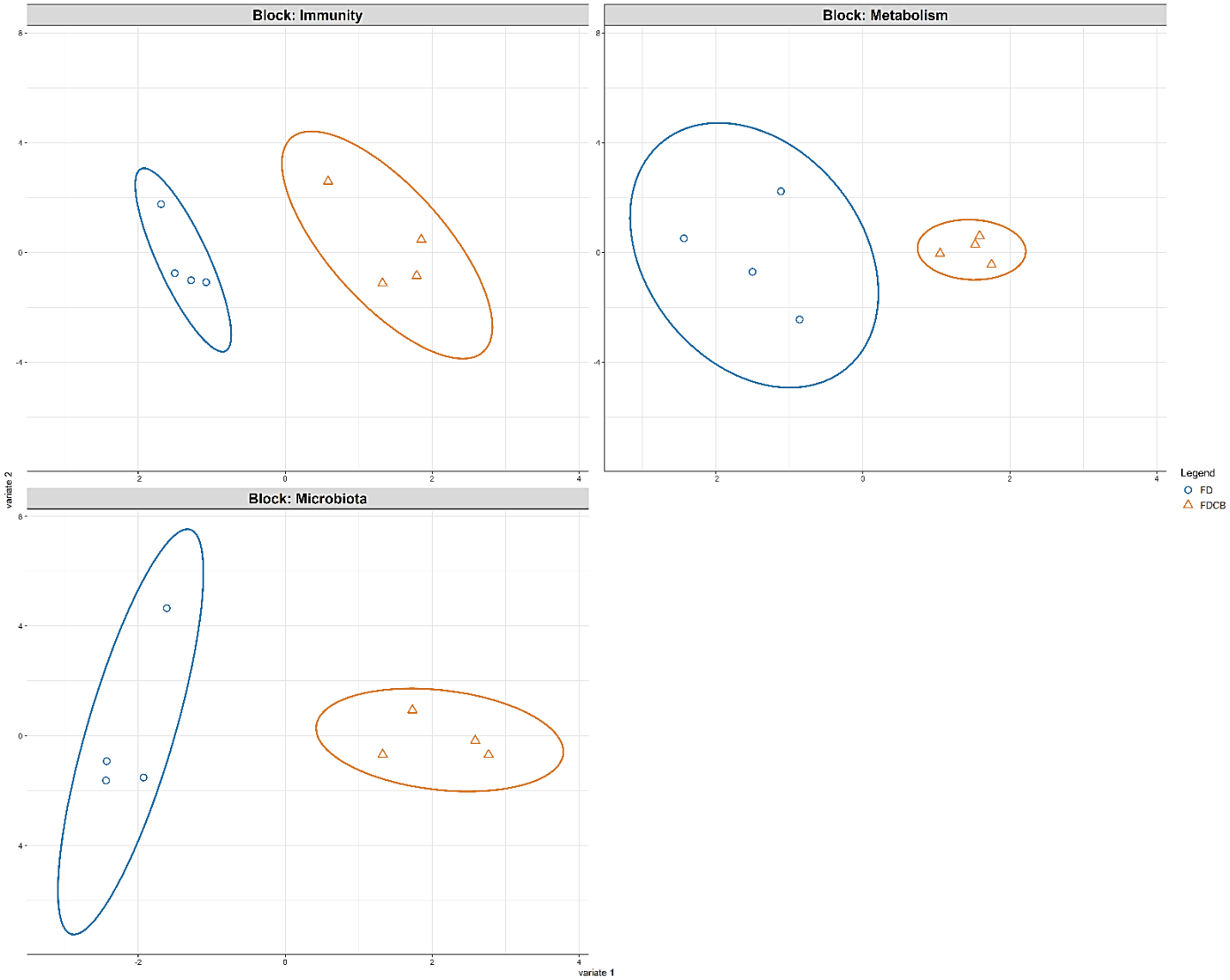

Supplementary Figure S1. *Figure X. Sample distribution by diet group across each data block from DIABLO analysis. Individual mice are projected onto the first two components of the model for immunity (top left), metabolism (top right), and microbiota (bottom left) datasets. Clear separation between FD (blue circles) and FDCB (orange triangles) groups was observed across all three blocks, indicating coordinated and diet-dependent multivariate signatures. Ellipses represent 95% confidence intervals.*

Supplementary Figure S2A. Variable contributions from each data block (microbiota, immunity, and metabolism) to the DIABLO integrative model components.

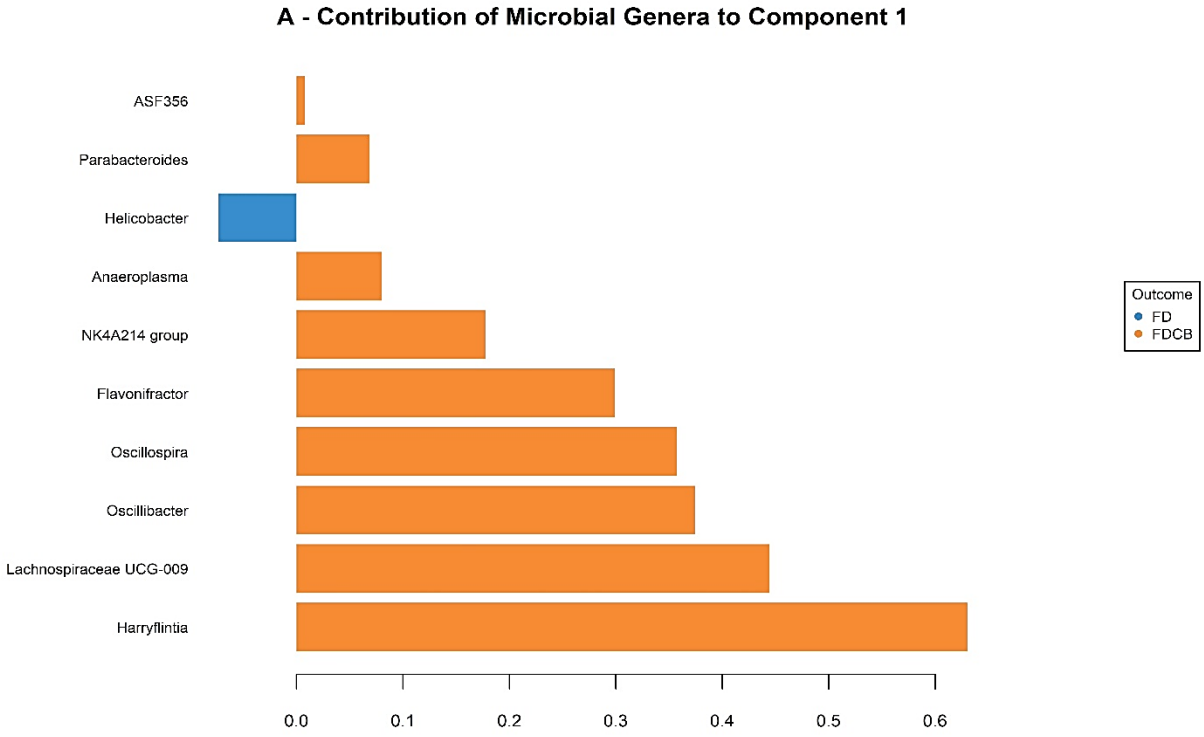

Supplementary Figure S2B.

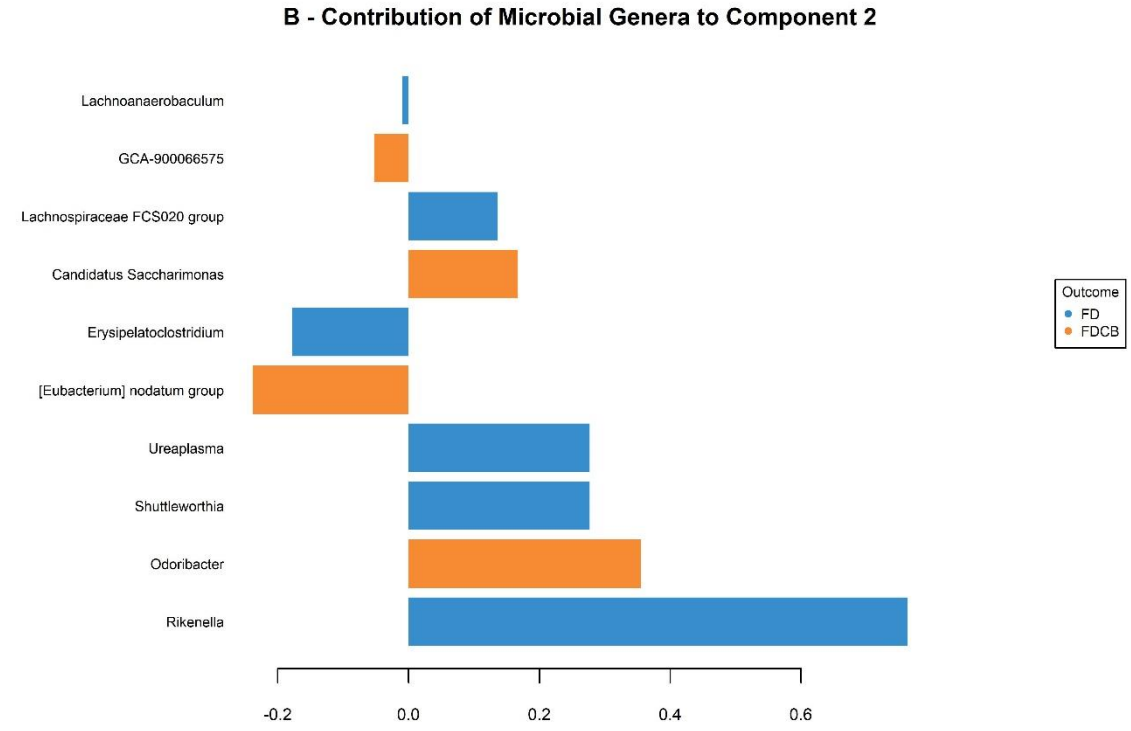

Supplementary Figure S2C.

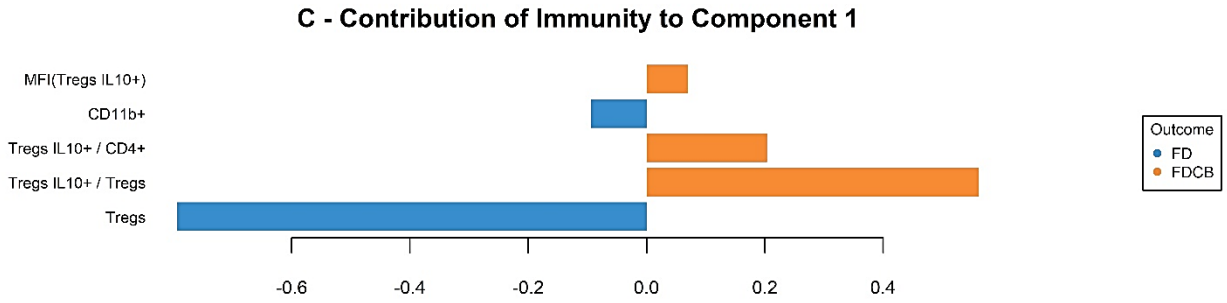

Supplementary Figure S2D.

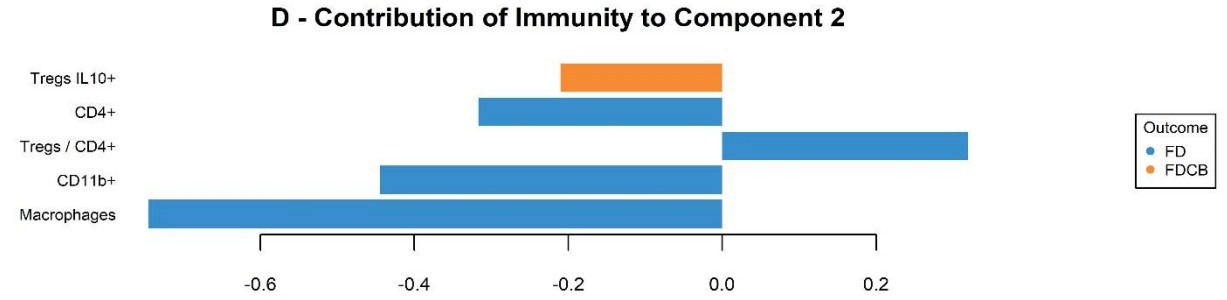

Supplementary Figure S2E.

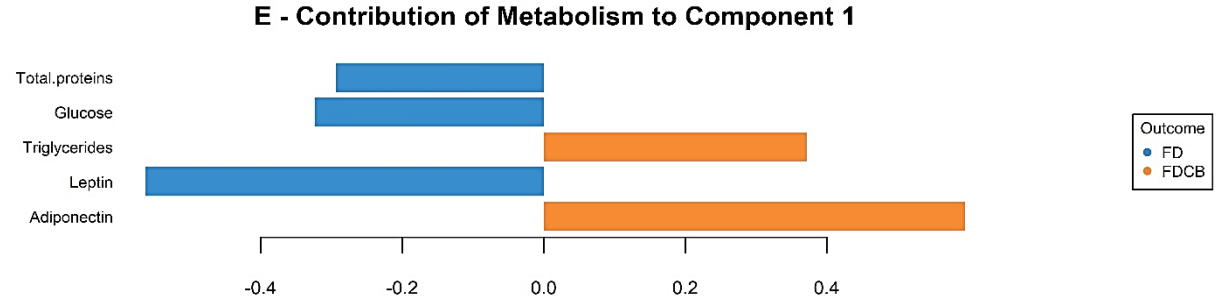

Supplementary Figure S2F.

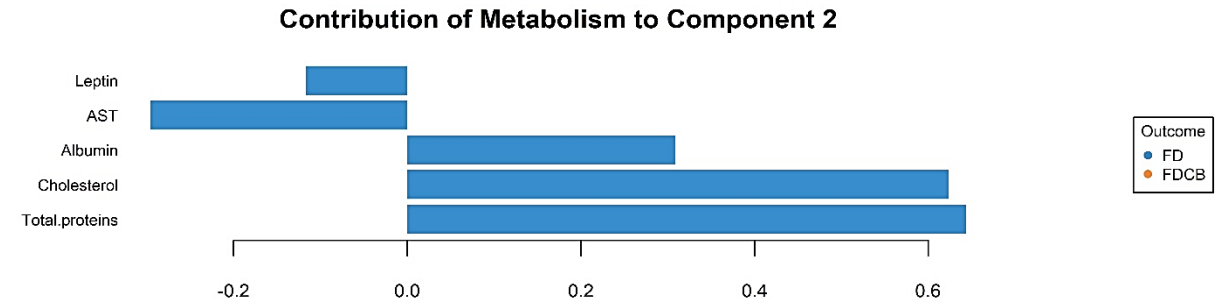

Supplementary Figure S2. *(A–B) Microbiota block: Barplots show the contribution of key microbial genera to Component 1 (A) and Component 2 (B). Genera such as Harryflintia, Oscillibacter, and Flavonifractor contributed most to Component 1, which distinguished the FDCB group, while Component 2 was driven by taxa enriched in FD. (C–D) Immunity block: Variables measured in visceral adipose tissue (VAT) contributing to Component 1 (C) and Component 2 (D) include regulatory T cell (Treg) subsets and myeloid populations. Component 1 highlighted Treg IL-10+ cells as major drivers in FDCB, while Component 2 captured shifts in CD11b+F4/80+ macrophages and total CD4+ T cells in FD. (E–F) Metabolism block: Metabolic variables contributing to Component 1 (E) and Component 2 (F). Component 1 is characterized by increased adiponectin and triglycerides in FDCB and elevated glucose, total proteins, and leptin in FD. Component 2 highlights FD-driven associations with serum cholesterol, albumin, AST, and total proteins.*

Author Contributions:

Conceptualization, N.D.P., R.C.C., and S.A.P.; methodology, N.D.P., N.E., G.B., Y.L.M. and R.C.C.; software, N.D.P. and N.E.; validation, N.D.P., R.C.C., and S.A.P.; formal analysis, N.D.P.; investigation, N.D.P. and S.A.P; resources, C.A.G., R.C.C., M.P.A., and S.A.P.; data curation, N.D.P; writing—original draft preparation, N.D.P. and S.A.P. ; writing—review and editing, C.A.G., R.C.C., M.P.A., and S.A.P.; visualization, N.D.P. and S.A.P.; supervision, R.C.C., M.P.A., and S.A.P.; project administration, R.C.C. and M.P.A.; funding acquisition, C.A.G., R.C.C., M.P.A., and S.A.P.. All authors have read and agreed to the published version of the manuscript.

Funding:

This work was supported in part by funding granted by Secretaría de Investigación y Vinculación Tecnológica from Universidad Católica de Córdoba. Accredited project: Nutritional Quality, a key factor that modulates the composition of the intestinal microbiota and the metabolic immune response in models of obesity. RR 2267-19. This work was supported in part by funding granted by Secretaría de Ciencia y Tecnología from Universidad Nacional de Córdoba (SECyT). Accredited projects: (A) Influence of nutritional quality, innate immunity, and acute infection with Trypanosoma cruzi in a diet-induced obesity model. Impact on development/ prevention of non-communicable chronic diseases. Amount Res. SECyT-UNC 411/2018. (B) Identification of mononuclear cell metabolic state in T. cruzi infection and its impact on the inflammatory response. SECyT-UNC 113/2018. This work was supported in part by LACE Laboratories SA.

Institutional Review Board Statement:

This research has the authorization of the Institutional Committee for the Care and Use of Laboratory—CICUAL-FCQ—Universidad Nacional de Córdoba, Córdoba, Argentina. RESOLUTION N° 939, EXP-UNC:0023836/2018.

Informed Consent Statement:

Not applicable.

Data Availability Statement:

Sequencing data are accessible in the National Center for Bio-technology Information (NCBI) database under BioProject accession number PRJNA1292224 (https://ncbi.nlm.nih.gov/bioproject/?term=PRJNA1292224)

Acknowledgments:

The authors acknowledge Eduardo Fernandez for continued support. The authors thank Pilar Crespo and Paula Abadie for the technical assistance at the CIBICI-CONICET FACS facility. M.P.A. is a member of the scientific community of Consejo Nacional de Investigaciones Científicas y Técnicas de la República Argentina (CONICET). Y.L.M. and G.B. thank CONICET for the fellowships.

Conflicts of Interest:

The authors declare no conflict of interest.

7. References:

1. Bray GA, Kim KK, Wilding JPH, World Obesity Federation. Obesity: a chronic relapsing progressive disease process. A position statement of the World Obesity Federation. *Obes Rev*. 2017;18(7):715-723. doi:10.1111/obr.12551

2. Weisberg SP, McCann D, Desai M, Rosenbaum M, Leibel RL, Ferrante AW. Obesity is associated with macrophage accumulation in adipose tissue. *J Clin Invest*. 2003;112(12):1796-1808. doi:10.1172/JCI200319246

3.Chait A, den Hartigh LJ. Adipose Tissue Distribution, Inflammation and Its Metabolic Consequences, Including Diabetes and Cardiovascular Disease. *Frontiers in Cardiovascular Medicine*. 2020;7. Accessed July 25, 2023. https://www.frontiersin.org/articles/10.3389/fcvm.2020.00022

4. Bradley D, Deng T, Shantaram D, Hsueh WA. Orchestration of the Adipose Tissue Immune Landscape by Adipocytes. Published online February 12, 2024. doi:10.1146/annurev-physiol-042222-024353

5. Castoldi A, Naffah de Souza C, Câmara NOS, Moraes-Vieira PM. The Macrophage Switch in Obesity Development. *Front Immunol*. 2016;6:637. doi:10.3389/fimmu.2015.00637

6. Feuerer M, Herrero L, Cipolletta D, et al. Lean, but not obese, fat is enriched for a unique population of regulatory T cells that affect metabolic parameters. *Nature Medicine*. 2009;15(8):930-939. doi:10.1038/nm.2002

7. Nishimura S, Manabe I, Nagasaki M, et al. CD8+ effector T cells contribute to macrophage recruitment and adipose tissue inflammation in obesity. *Nat Med*. 2009;15(8):914-920. doi:10.1038/nm.1964

8. Zatterale F, Longo M, Naderi J, et al. Chronic Adipose Tissue Inflammation Linking Obesity to Insulin Resistance and Type 2 Diabetes. *Front Physiol*. 2020;10:1607. doi:10.3389/fphys.2019.01607

9. Agans R, Gordon A, Kramer DL, Perez-Burillo S, Rufián-Henares JA, Paliy O. Dietary Fatty Acids Sustain the Growth of the Human Gut Microbiota. *Appl Environ Microbiol*. 2018;84(21):e01525-18. doi:10.1128/AEM.01525-18

10. Daniel H, Gholami AM, Berry D, et al. High-fat diet alters gut microbiota physiology in mice. *ISME J*. 2014;8(2):295-308. doi:10.1038/ismej.2013.155

11. Shen W, Gaskins HR, McIntosh MK. Influence of dietary fat on intestinal microbes, inflammation, barrier function and metabolic outcomes. *J Nutr Biochem*. 2014;25(3):270-280. doi:10.1016/j.jnutbio.2013.09.009

12. Xu AA, Kennedy LK, Hoffman K, et al. Dietary Fatty Acid Intake and the Colonic Gut Microbiota in Humans. *Nutrients*. 2022;14(13):2722. doi:10.3390/nu14132722

13. Schoeler M, Caesar R. Dietary lipids, gut microbiota and lipid metabolism. *Rev Endocr Metab Disord*. 2019;20(4):461-472. doi:10.1007/s11154-019-09512-0

14. Portela ND, Galván C, Sanmarco LM, et al. Omega-3-Supplemented Fat Diet Drives Immune Metabolic Response in Visceral Adipose Tissue by Modulating Gut Microbiota in a Mouse Model of Obesity. *Nutrients*. 2023;15(6):1404. doi:10.3390/nu15061404

15. Portela ND, Eberhardt N, Bergero G, et al. Dietary Omega-3 Supplementation Shapes Gut Microbiota and Regulates Immunometabolism in a Mouse Model of Obesity. *Medical Research Archives*. 2025;13(5). doi:10.18103/mra.v13i5.6623

16. Choi SW, Friso S. Modulation of DNA methylation by one-carbon metabolism: a milestone for healthy aging. *Nutr Res Pract*. 2023;17(4):597-615. doi:10.4162/nrp.2023.17.4.597

17. Sivanesan S, Taylor A, Zhang J, Bakovic M. Betaine and Choline Improve Lipid Homeostasis in Obesity by Participation in Mitochondrial Oxidative Demethylation. *Front Nutr*. 2018;5:61. doi:10.3389/fnut.2018.00061

18. Chen Q, Wang Y, Jiao F, et al. Betaine inhibits Toll-like receptor 4 responses and restores intestinal microbiota in acute liver failure mice. *Scientific Reports*. 2020;10(1):21850. doi:10.1038/s41598-020-78935-6

19. Zhao G, He F, Wu C, et al. Betaine in Inflammation: Mechanistic Aspects and Applications. *Front Immunol*. 2018;9:1070. doi:10.3389/fimmu.2018.01070

20. Ellacott KLJ, Morton GJ, Woods SC, Tso P, Schwartz MW. Assessment of feeding behavior in laboratory mice. *Cell Metab*. 2010;12(1):10-17. doi:10.1016/j.cmet.2010.06.001

21. Callahan BJ, McMurdie PJ, Rosen MJ, Han AW, Johnson AJA, Holmes SP. DADA2: High resolution sample inference from Illumina amplicon data. *Nat Methods*. 2016;13(7):581-583. doi:10.1038/nmeth.3869

22. McMurdie PJ, Holmes S. phyloseq: An R Package for Reproducible Interactive Analysis and Graphics of Microbiome Census Data. *PLOS ONE*. 2013;8(4):e61217. doi:10.1371/journal.pone.0061217

23. Leo Lahti SS. microbiome R package. Published online 2019 2012. http://microbiome.github.io

24. Quast C, Pruesse E, Yilmaz P, et al. The SILVA ribosomal RNA gene database project: improved data processing and web-based tools. *Nucleic Acids Research*. 2013;41(D1):D590-D596. doi:10.1093/nar/gks1219

25. R Core Team. R Core Team (2022). R: A language and environment for statistical computing. Published online 2021. https://www.R-project.org/.

26. Wickham H. ggplot2: Elegant Graphics for Data Analysis. 2016. Accessed January 25, 2023. https://link.springer.com/book/10.1007/978-3-319-24277-4

27. Kassambara A. ggpubr: "ggplot2" Based Publication Ready Plots. R package version 0.5.0. Published online 2022. https://CRAN.R-project.org/package=ggpubr

28. Cao Y, Dong Q, Wang D, Zhang P, Liu Y, Niu C. microbiomeMarker: an R/Bioconductor package for microbiome marker identification and visualization. *Bioinformatics*. 2022;38(16):4027-4029. doi:10.1093/b ioinformatics/btac438

29. Wei T SV. R package "corrplot": Visualization of a Correlation Matrix. Published online 2021. https://github.com/taiyun/corrplot.

30. Rohart F, Gautier B, Singh A, Cao KAL. mixOmics: An R package for 'omics feature selection and multiple data integration. Published online 2017. doi:10.1371/journal.pcbi.1005752

31. Hu H, Tan L, Li X, et al. Betaine Reduces Lipid Anabolism and Promotes Lipid Transport in Mice Fed a High-Fat Diet by Influencing Intestinal Protein Expression. *Foods*. 2022;11(16):2421. doi:10.3390/foods11162421

32. Wang X, Shang X, Pan Y, Fu Y, Zhu H, Yan S. Frontiers | Betaine alleviates obesity-related metabolic disorders in rats: insights from microbiomes, lipidomics, and transcriptomics. Published online 2025. doi:10.3389/fnut.2025.1604801

33. Kathirvel E, Morgan K, Malysheva OV, Caudill MA, Morgan TR. Betaine for the prevention and treatment of insulin resistance and fatty liver in a high-fat dietary model of insulin resistance in C57BL mice. *Front Nutr*. 2024;11:1409972. doi:10.3389/fnut.2024.1409972

34. Zeng Q, Zhao M, Wang F, et al. Integrating Choline and Specific Intestinal Microbiota to Classify Type 2 Diabetes in Adults: A Machine Learning Based Metagenomics Study. *Front Endocrinol (Lausanne)*. 2022;13:906310. doi:10.3389/fendo.2022.906310

35. Corbin KD, Zeisel SH. Choline Metabolism Provides Novel Insights into Non-alcoholic Fatty Liver Disease and its Progression. *Curr Opin Gastroenterol*. 2012;28(2):159-165. doi:10.1097/MOG.0b013e32834e7b4b

36. Arpaia N, Campbell C, Fan X, et al. Metabolites produced by commensal bacteria promote peripheral regulatory T-cell generation. *Nature*. 2013;504(7480):451-455. doi:10.1038/nature12726

37. Sun M, Wu W, Chen L, et al. Microbiota-derived short-chain fatty acids promote Th1 cell IL-10 production to maintain intestinal homeostasis. *Nat Commun*. 2018;9(1):3555. doi:10.1038/s41467-018-05901-2

38. Chen L, Sun M, Wu W, et al. Microbiota Metabolite Butyrate Differentially Regulates Th1 and Th17 Cells' Differentiation and Function in Induction of Colitis. *Inflamm Bowel Dis*. 2019;25(9):1450-1461. doi:10.1093/ibd/izz046

39. Romano KA, Campo AM del, Kasahara K, et al. Metabolic, Epigenetic, and Transgenerational Effects of Gut Bacterial Choline Consumption. *Cell Host Microbe*. 2017;22(3):279-290.e7. doi:10.1016/j.chom.2017.07.021

40. Kropp C, Le Corf K, Relizani K, et al. The Keystone commensal bacterium Christensenella minuta DSM 22607 displays anti-inflammatory properties both in vitro and in vivo. *Sci Rep*. 2021;11:11494. doi:10.1038/s41598-021-90885-1

41. Tavella T, Rampelli S, Guidarelli G, et al. Elevated gut microbiome abundance of Christensenellaceae, Porphyromonadaceae and Rikenellaceae is associated with reduced visceral adipose tissue and healthier metabolic profile in Italian elderly. *Gut Microbes*. 2021;13(1):1880221. doi:10.1080/19490976.2021.1880221

42. Yang J, Li Y, Wen Z, Liu W, Meng L, Huang H. Oscillospira - a candidate for the next-generation probiotics. *Gut Microbes*. 2021;13(1):1987783. doi:10.1080/19490976.2021.1987783

43. Cui Y, Zhang L, Wang X, et al. Roles of intestinal Parabacteroides in human health and diseases. *FEMS Microbiology Letters*. 2022;369(1):fnac072. doi:10.1093/femsle/fnac072

44. Wang K, Liao M, Zhou N, et al. Parabacteroides distasonis Alleviates Obesity and Metabolic Dysfunctions via Production of Succinate and Secondary Bile Acids. Published online 2019. Accessed July 16, 2025. https://www.cell.com/cell-reports/abstract/S2211-1247(18)31958-2

45. Parker BJ, Wearsch PA, Veloo ACM, Rodriguez-Palacios A. The Genus Alistipes: Gut Bacteria With Emerging Implications to Inflammation, Cancer, and Mental Health. *Frontiers in Immunology*. 2020;11. Accessed February 18, 2024. https://www.frontiersin.org/journals/immunology/articles/10.3389/fimmu.2020.00906

46. López-Montoya P, Rivera-Paredez B, Palacios-González B, et al. Dietary Patterns Are Associated with the Gut Microbiome and Metabolic Syndrome in Mexican Postmenopausal Women. *Nutrients*. 2023;15(22):4704. doi:10.3390/nu15224704

47. Kountouras J, Papaefthymiou A, Polyzos SA, et al. Impact of Helicobacter pylori-Related Metabolic Syndrome Parameters on Arterial Hypertension. *Microorganisms*. 2021;9(11):2351. doi:10.3390/microorganisms9112351

48. Koeth RA, Wang Z, Levison BS, et al. Intestinal microbiota metabolism of L-carnitine, a nutrient in red meat, promotes atherosclerosis. *Nat Med*. 2013;19(5):576-585. doi:10.1038/nm.3145

49. Wang Z, Klipfell E, Bennett BJ, et al. Gut flora metabolism of phosphatidylcholine promotes cardiovascular disease. *Nature*. 2011;472(7341):57-63. doi:10.1038/nature09922

50. Romano KA, Vivas EI, Amador-Noguez D, Rey FE. Intestinal Microbiota Composition Modulates Choline Bioavailability from Diet and Accumulation of the Proatherogenic Metabolite Trimethylamine-N-Oxide. *mBio*. 2015;6(2):10.1128/mbio.02481-14. doi:10.1128/mbio.02481-14

51. Kuerbanjiang M, Yu W, Shang T, et al. Association between dietary betaine intake and overweight or obesity. *Sci Rep*. 2024;14:32031. doi:10.1038/s41598-024-83646-3

